



# Altered Extracellular Vesicle Concentration, Cargo, and Function in Diabetes

David W. Freeman,<sup>1</sup> Nicole Noren Hooten,<sup>1</sup> Erez Eitan,<sup>2</sup> Jamal Green,<sup>1</sup> Nicolle A. Mode,<sup>1</sup> Monica Bodogai,<sup>3</sup> Yongqing Zhang,<sup>4</sup> Elin Lehrmann,<sup>4</sup> Alan B. Zonderman,<sup>1</sup> Arya Biragyn,<sup>3</sup> Josephine Egan,<sup>5</sup> Kevin G. Becker,<sup>4</sup> Mark P. Mattson,<sup>2</sup> Ngozi Ejiogu,<sup>1</sup> and Michele K. Evans<sup>1</sup>

*Diabetes* 2018;67:2377–2388 | <https://doi.org/10.2337/db17-1308>

**Type 2 diabetes is a chronic age-associated degenerative metabolic disease that reflects relative insulin deficiency and resistance. Extracellular vesicles (EVs) (exosomes, microvesicles, and apoptotic bodies) are small (30–400 nm) lipid-bound vesicles capable of shuttling functional proteins, nucleic acids, and lipids as part of intercellular communication systems. Recent studies in mouse models and in cell culture suggest that EVs may modulate insulin signaling. Here, we designed cross-sectional and longitudinal cohorts of euglycemic participants and participants with prediabetes or diabetes. Individuals with diabetes had significantly higher levels of EVs in their circulation than euglycemic control participants. Using a cell-specific EV assay, we identified that levels of erythrocyte-derived EVs are higher with diabetes. We found that insulin resistance increases EV secretion. Furthermore, the levels of insulin signaling proteins were altered in EVs from individuals with high levels of insulin resistance and  $\beta$ -cell dysfunction. Moreover, EVs from individuals with diabetes were preferentially internalized by circulating leukocytes. Cytokine levels in the media and in EVs were higher from monocytes incubated with diabetic EVs. Microarray of these leukocytes revealed altered gene expression pathways related to cell survival, oxidative stress, and immune function. Collectively, these results suggest that insulin resistance increases the secretion of EVs, which are preferentially internalized by leukocytes, and alters leukocyte function.**

One of the most important medical challenges is the epidemic of type 2 diabetes. It is estimated that 9.4% of the U.S. population (~30 million) is affected by this disease (1), while older individuals and different racial groups are affected disproportionately. Individuals with diabetes have an increased risk for age-associated comorbidities including hypertension, dementia, renal disease, and chronic heart disease (2). Therefore, it is important to understand how diabetes contributes to the development and severity of these age-associated diseases. Furthermore, individuals with diabetes have impaired cellular insulin signaling, and accumulating data suggest that circulating factors may also contribute to the disease.

Recent data indicate that membrane-bound extracellular vesicles (EVs) (30–400 nm) are important mediators of intercellular communication among different tissues and organs. EVs, found in most bodily fluids, contain proteins, RNA, and lipids and can be characterized into at least one of three groups. Exosomes are released through the fusion of multivesicular bodies with the plasma membrane. Microvesicles are released by budding of the plasma membrane, and apoptotic bodies are shed from dying cells (3). EVs have a role in physiological and pathological intercellular signaling and in a wide spectrum of biological functions (3).

While EVs have been studied in the context of many diseases (4), little is known about EVs in the context of human diabetes. Studies in the *db/db* diabetic mouse model

<sup>1</sup>Laboratory of Epidemiology and Population Science, National Institute on Aging, National Institutes of Health, Baltimore, MD

<sup>2</sup>Laboratory of Neuroscience, National Institute on Aging, National Institutes of Health, Baltimore, MD

<sup>3</sup>Laboratory of Molecular Biology and Immunology, National Institute on Aging, National Institutes of Health, Baltimore, MD

<sup>4</sup>Laboratory of Genetics and Genomics, National Institute on Aging, National Institutes of Health, Baltimore, MD

<sup>5</sup>Laboratory of Clinical Investigation, National Institute on Aging, National Institutes of Health, Baltimore, MD

Corresponding author: Michele K. Evans, [me42v@nih.gov](mailto:me42v@nih.gov).

Received 27 October 2017 and accepted 20 April 2018.

This article contains Supplementary Data online at <http://diabetes.diabetesjournals.org/lookup/suppl/doi:10.2337/db17-1308/-/DC1>.

D.W.F. and N.N.H. contributed equally to this work.

© 2018 by the American Diabetes Association. Readers may use this article as long as the work is properly cited, the use is educational and not for profit, and the work is not altered. More information is available at <http://www.diabetesjournals.org/content/license>.

See accompanying article, p. 2154.

demonstrated that EVs from adipose tissue activate macrophages and promote expression of IL-6 and TNF- $\alpha$  (5), suggesting that EVs from diabetic mice may convey inflammatory signals. EVs from insulin resistant mice modulate insulin signaling in skeletal muscle (6) and pancreatic  $\beta$ -cells (7), further suggesting a role for EVs in insulin signaling in mice. Recent evidence shows that in adipose tissue, macrophage-derived exosomes may modulate insulin resistance in mice through transfer of specific microRNAs (8).

Studies investigating the interplay between EVs and diabetes in humans have been predominantly in vitro studies. EVs derived from adipocyte cell lines or explants *ex vivo* were incubated with a hepatocyte and skeletal muscle cell line. However, the results have not confirmed the effects on insulin signaling (9). Additionally, EVs from human adipocyte explants have been shown to modulate the release of inflammatory cytokines in macrophages (10).

Thus far, human data have primarily investigated the relationship between larger microparticles isolated at slow centrifugation speeds or by FACS (11) and type 2 diabetes (12–14). For example, circulating endothelium-derived microparticles (15) increase with type 2 diabetes (12–14). However, EVs in the circulation are derived from many different cell types and vary extensively in size. Specifically, EVs encompassing the size range of exosomes, microvesicles, and apoptotic bodies have not been investigated extensively in the context of diabetes in humans.

To investigate whether these previously reported changes *in vitro* and in animal models were consistent with changes in individuals with diabetes, we examined different EV characteristics in cross-sectional and longitudinal cohorts of both euglycemic individuals and individuals with diabetes.

## RESEARCH DESIGN AND METHODS

### Clinical Study Participants

Three subcohorts of euglycemic individuals and individuals with diabetes were selected from the Healthy Aging in Neighborhoods of Diversity across the Life Span (HANDLS)

study of the National Institute on Aging (NIA) Intramural Research Program, National Institutes of Health (NIH). HANDLS has been approved by the institutional review board of the National Institute of Environmental Health Science, NIH. All participants provided written informed consent. HANDLS is a longitudinal study comprised of community-dwelling participants investigating the role of race and socioeconomic status in the development of age-associated health disparities. Individuals with diabetes met one of the following three criteria: 1) previous diagnosis by health care provider, 2) currently taking medication for diabetes, or 3) fasting serum glucose >125 mg/dL. Plasma samples were collected after overnight fasting.

Cross-sectional cohort 1 was comprised of 16 euglycemic individuals and 22 individuals with diabetes, and cross-sectional cohort 2 comprised obesity-matched euglycemic individuals and individuals with diabetes ( $n = 30$ /group) (Table 1 and Fig. 1A and B). Individuals were classified based on BMI as underweight/normal (<25 kg/m<sup>2</sup>), overweight (25 to <30 kg/m<sup>2</sup>), obese class I (30 to <35 kg/m<sup>2</sup>), and obese class II/III ( $\geq 35$  kg/m<sup>2</sup>). Underweight and normal individuals were grouped together owing to a low number of underweight participants. We chose 58 obesity-matched individuals for the longitudinal cohort who had blood samples two times  $\sim 5$  years apart ( $4.95 \pm 0.23$ ) and who were grouped as follows: euglycemia at both times ( $n = 19$ ), euglycemia at time 1 and diabetes at time 2 ( $n = 19$ ), and prediabetes at time 1 and diabetes at time 2 ( $n = 20$ ) (Table 2 and Fig. 1C).

HOMA of  $\beta$ -cell function (HOMA-B) and HOMA of insulin resistance (HOMA-IR) were calculated based on fasting serum glucose and fasting insulin levels (16) and were divided into quintiles for our analysis.

### ExoQuick EV Isolation

A fasting plasma sample was obtained as previously described (17). Plasma EVs were isolated from either 0.5 mL or 0.25 mL (cross-sectional cohort 2) using ExoQuick Exosome precipitation solution (System Biosciences) as previously described (17) and resuspended in either 0.5 mL

**Table 1—Clinical characteristics of cross-sectional cohorts**

	Cross-sectional cohort 1			Cross-sectional cohort 2		
	Euglycemia	Diabetes	<i>P</i>	Euglycemia	Diabetes	<i>P</i>
<i>N</i>	16	22		30	30	
Age, years	53.79 (10.72)	56.10 (9.86)	0.498	47.81 (11.65)	55.14 (6.99)	0.005
BMI, kg/m <sup>2</sup>	25.41 (4.19)	39.16 (9.33)	<0.001	35.01 (7.49)	35.45 (6.64)	0.811
Glucose, mg/dL	91.80 (5.25)	161.05 (88.32)	0.005	92.37 (5.65)	165.60 (71.64)	<0.001
LDL, mg/dL	112.33 (37.88)	108.18 (37.72)	0.745	108.77 (40.34)	108.80 (43.21)	0.998
HDL, mg/dL	55.40 (11.34)	45.82 (11.13)	0.015	50.67 (11.46)	44.70 (13.23)	0.067
Nonsmoking, <i>n</i> (%)	12 (75.0)	13 (65.0)	0.777	15 (57.7)	24 (88.9)	0.024
AA race, <i>n</i> (%)	6 (37.5)	10 (45.5)	0.875	20 (66.7)	19 (63.3)	1.000
Women, <i>n</i> (%)	9 (56.2)	14 (63.6)	0.901	20 (66.7)	15 (50.0)	0.295

Mean (SD) is shown for continuous variables and analyzed by one-way ANOVA, unless otherwise indicated.  $\chi^2$  goodness-of-fit test was used to analyze differences for categorical variables. AA, African American.

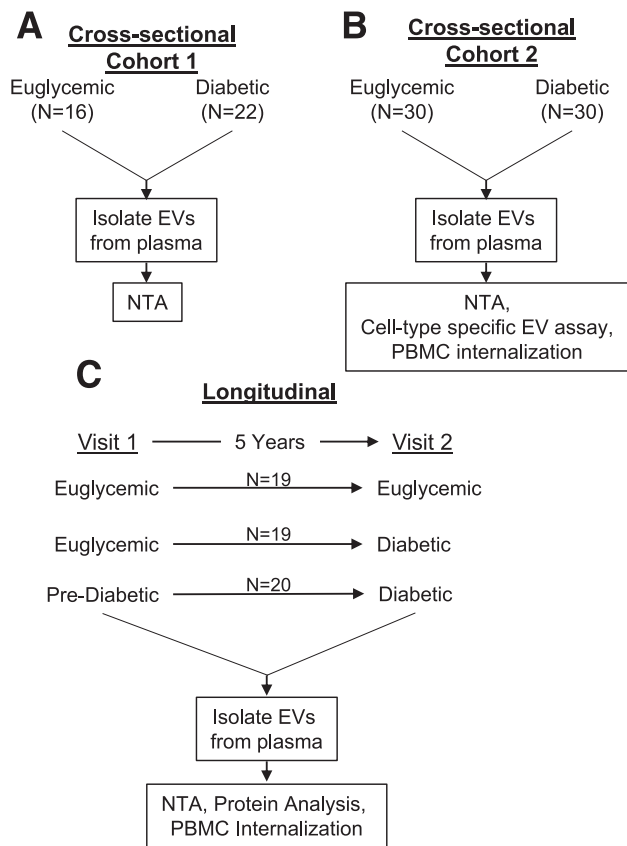


**Figure 1**—Cohort design. *A* and *B*: Cross-sectional cohorts 1 and 2 of euglycemic individuals and individuals with diabetes. *C*: Longitudinal cohort design of euglycemic individuals and individuals with prediabetes or diabetes.

or 0.25 mL, respectively. This isolation method provides more reproducible results than either differential ultracentrifugation or size exclusion columns (17) and also is more suitable for EV isolation from large human cohorts.

#### Differential Ultracentrifugation EV Isolation

EVs were isolated from plasma and conditioned media via differential ultracentrifugation as previously described (18). Media was centrifuged at 500g for 10 min, at 2,500g for 10 min, and then at 120,000g for 2 h in a Beckman ultracentrifugation (SW 32 Ti rotor, K = 204). Resuspended pellet was transferred to a new tube and centrifuged at 120,000g for 2 h (SW 55 Ti rotor, K = 48). Plasma EVs were isolated using the same protocol with the following modification. Following centrifugation at 2,500g, the supernatant was centrifuged at 10,000g for 30 min. The supernatant was then subjected to two ultracentrifugation spins at 120,000g as described above. The 10,000g pellet was resuspended in PBS and centrifuged at 10,000g for 30 min.

#### Immunoblotting

EV (10  $\mu$ g) samples lysed in mammalian protein extraction reagent (M-PER), 3T3-L1 preadipocyte cell line lysate, and

two plasma ExoQuick EV-depleted supernatant samples were subjected to SDS-PAGE and immunoblotted with antibodies from Abcam, TSG101 [clone EPR7131(B)], FLOT1 (clone EPR6041), and Calnexin (ab22595), and from Santa Cruz Biotechnologies, ALIX (clone C-11). Neuronal cell lysates were immunoblotted with antibodies to phospho-AKT (Clone D9E, Cell Signaling), AKT (clone C67E7, Cell Signaling), and actin (ab8226, Abcam).

#### Electron Microscopy

Electron microscopy was performed by the Johns Hopkins University Neurology Microscopy Core as described (17). Grids were viewed on a Libra 120 TEM at 120 Kv (Zeiss). Images were taken with a Veleta camera (Olympus).

#### Nanoparticle Tracking Analysis

Isolated EV samples were diluted 1:300 and 1:50 in 0.2  $\mu$ mol/L filtered PBS for EVs isolated by ExoQuick and differential ultracentrifugation, respectively. Size distribution and concentration were analyzed using nanoparticle tracking analysis (NTA) on a NanoSight NS500 (Malvern Instruments). Samples were recorded at camera level 14, detection level 3, and five videos of 20 s with a coefficient of variance <20% were used for analysis. To ensure measurement accuracy, we ensured that all samples were analyzed during the same time frame for each cohort/experiment on a single instrument by the same operator. All analyses were performed with blinding to disease status. Total EV concentration from plasma was calculated as previously described (17).

#### Cell-Specific EV Assay

Streptavidin-coated black plates (Thermo Fisher) were coated with biotin-labeled primary antibodies (5  $\mu$ g/mL) against CD62p (304914; BioLegend), CD68 (333804; BioLegend), CD235a (13-9987-82; Thermo Fisher), (ab77928; Abcam), and IgG1, $\kappa$  Isotype control (400103; BioLegend) in PBS/0.5% BSA at 4°C overnight. After blocking in PBS/5% BSA, plates were washed with PBS. Plasma EVs from cross-sectional cohort 2 were labeled with 0.1  $\mu$ mol/L (final concentration) PKH26 (category no. 1077; Sigma-Aldrich) and excess dye was removed as previously described (17). The remaining volume (150  $\mu$ L) was diluted 1:3 in PBS, and 40  $\mu$ L was added to each well and incubated for 2 h at room temperature. After washing three times with PBS, the PKH26 signal was read by a fluorescent plate reader (excitation 540 nm and emission 570 nm). Each sample was performed in duplicate, and the average intensity was used for analysis.

#### Primary Neuronal Cell Culture

Cortical neurons were dissected from embryonic Sprague-Dawley rats (E18) (Animal Protocol no. 263-LNS-2019) as previously described (19). This research was approved by the NIA Animal Care and Use Committee and was performed according to guidelines in the NIH Guide for the Care and Use of Laboratory Animals. Cells were

**Table 2—Clinical characteristics of longitudinal cohort**

	Time	NoDx→NoDx	NoDx→DM	PreDM→DM	<i>P</i>
<i>N</i>		19	19	20	
Age, years	Time 1	42.50 (8.26)	47.84 (8.58)	47.69 (8.68)	0.095
	Time 2	47.60 (8.75)	52.76 (8.50)	52.21 (8.84)	0.141
BMI, kg/m <sup>2</sup>	Time 1	33.10 (5.60)	35.40 (7.66)	35.56 (9.11)	0.540
	Time 2	33.92 (5.48)	36.63 (9.41)	35.44 (8.63)	0.585
Glucose, mg/dL	Time 1	89.42 (4.14)	93.26 (9.13)	110.55 (6.06)	<0.001
	Time 2	89.58 (6.13)	125.53 (40.68)	131.55 (45.81)	0.001
LDL, mg/dL	Time 1	132.63 (38.20)	133.05 (31.06)	118.45 (32.13)	0.315
	Time 2	123.53 (33.66)	119.42 (37.89)	119.15 (36.06)	0.915
HDL, mg/dL	Time 1	50.95 (14.25)	50.05 (11.97)	42.55 (10.21)	0.070
	Time 2	55.84 (11.55)	53.47 (15.21)	44.80 (11.01)	0.022
Nonsmoking, <i>n</i> (%)	Time 1	5 (50.0)	6 (33.3)	10 (55.6)	0.389
	Time 2	5 (35.7)	8 (50.0)	8 (44.4)	0.783
White race, <i>n</i> (%)		7 (36.8)	5 (26.3)	8 (40.0)	0.645
Women, <i>n</i> (%)		14 (73.7)	12 (63.2)	14 (70)	0.776

Mean (SD) is shown for continuous variables and analyzed by one-way ANOVA, unless otherwise indicated.  $\chi^2$  goodness-of-fit test was used to analyze differences for categorical variables. DM, diabetes; NoDx, euglycemia; PreDM, prediabetes.

maintained in Neuralbasal medium containing 1 mmol/L *d*-glucose and B27 without insulin (Thermo Scientific). On either day in vitro six or seven, cells were treated with either media containing 200 nmol/L Novolin R100 insulin or no insulin for 48 or 24 h. Media was collected and fresh media either containing 200 nmol/L insulin or no insulin was added for 30 min, after which media was collected. Wortmannin was added for both the 24 h and 30 min time points. Cells were washed with PBS, collected, and pelleted at 500g for 10 min and lysed with M-PER.

### ELISAs

Equal volumes of lysed EVs were used for quantitative protein measurement by the following Meso Scale kits (Meso Scale Discovery): Insulin Signaling Panel Phospho Protein (category no. K15151A-1), AKT Signaling Panel Whole Cell Lysate kit (category no. K15177D-1), and Phospho-IRS-1 Base kit (category no. 150HLA-1). Leptin receptor was analyzed by a kit from R&D Systems (category no. DY389).

### Peripheral Blood Mononuclear Cell Internalization Assay

Human peripheral blood was collected by the Health Apheresis Unit and the Clinical Core Laboratory, the NIA, under Human Subject and Tissue Procurement protocols. All participants provided written consent, and the protocols have been approved by the institutional review board of the National Institute of Environmental Health Sciences, NIH.

Peripheral blood mononuclear cells (PBMCs) were incubated with PKH26-labeled plasma EVs for 24 h, and cells were sorted as previously described (17). For the experiments in Fig. 5 and Supplementary Fig. 3, two PBMC donors were used, aged 47 and 60, respectively. They were both female and without allergies, and one was a smoker.

For gene expression changes, PBS or PKH26-labeled EVs from individuals with diabetes or euglycemic individuals were pooled together and incubated with PBMCs (female and 38 years old with no allergies) for 24 h. After the incubation, monocytes were isolated using the Monocyte Isolation Kit II (Miltenyi Biotec). RNA was isolated with TRIzol Reagent (Thermo Fisher Scientific) including a DNase treatment.

### Microarray and Quantitative RT-PCR

Total RNA quantity and quality were tested using the Agilent Bioanalyzer RNA 6000 Chip (Agilent, Santa Clara, CA). Monocyte gene expression was analyzed by microarray using Illumina HumanHT-12 v4 (Illumina, San Diego, CA). Microarray was performed and analyzed as previously described (20) and is available at Gene Expression Omnibus accession number: GSE105167.

For real-time quantitative RT-PCR (qRT-PCR) analysis, two PBMC donors were used aged 38 and 46 years. They were both female, without allergies, and one was a smoker. PBMCs were incubated for 6 h with euglycemic or diabetic EVs pooled from donors from cross-sectional cohort 2. Monocytes were sorted as described above and then incubated in media containing EV-depleted FBS (17). After 12 h, media and monocytes were separated by centrifuging at 500g. Monocyte total RNA was isolated and reverse transcribed using random hexamers, and real-time qRT-PCR was performed using gene-specific primers (Supplementary Table 1) and SYBR green master mix on a 7900HT Fast Real-Time PCR System (Applied Biosystems). Gene expression was normalized to the average of *HPRT* and *UBC*.

Media from the processes described above was collected after the 2,500g centrifugation, and EVs were then isolated by ultracentrifugation and lysed in M-PER. Cytokines from EVs and media were measured on a Human Proinflammatory

Panel I (K15049D; MesoScale Diagnostics) according to the manufacturer's instructions.

### Statistics

Statistical analyses were performed using R, version 3.3.2 (21). Concentration values were positively skewed and thus log (natural logarithm) transformed for testing in linear models. ANOVA was used to test the mean log concentration for the cross-sectional cohort. Linear mixed models, accounting for the matching across BMI groups, were used to examine the longitudinal cohort and included age, sex, and race.

## RESULTS

### Higher EV Concentration With Type 2 Diabetes

To assess differences in circulating EVs with type 2 diabetes, we designed cross-sectional and longitudinal cohorts of both euglycemic individuals and individuals with diabetes (Tables 1 and 2 and Fig. 1). Isolated plasma EVs were validated according to the International Society of Extracellular Vesicles guidelines (22). Known EV markers were present in each of the EV samples and absent in EV-depleted plasma (Fig. 2A). The electron microscopy image shows intact, round vesicles of ~50–200 nm (Fig. 2B). A similar size distribution was also confirmed by NTA with a peak around 175 nm (Fig. 2B and C). These data confirm the size, morphology, and protein markers that are characteristic of EVs.

We sought to determine whether there were differences in plasma EV concentration and size between euglycemic individuals and individuals with diabetes. An analysis of a cross-sectional cohort consisting of both groups revealed a significantly higher EV concentration in individuals with diabetes compared with euglycemic individuals ( $P = 0.022$  [Fig. 2D]). To further validate these results and to exclude the possibility that obesity contributes to higher EV levels in individuals with diabetes, we designed a second cross-sectional cohort matched on obesity status (Table 1). A linear mixed model regression analysis of EV concentration revealed a significant interaction between diabetes and race, such that individuals with diabetes had significantly higher levels of circulating EVs than euglycemic individuals among white participants (Fig. 2E).

Although lipoproteins may coprecipitate with EVs, the significant relationship of diabetes and race for EV concentration was unaffected by LDL or HDL levels in the model. This suggests that the relationship between diabetes and EV concentration is stronger than what could be explained by differences between lipoprotein levels. Additionally, neither HDL nor LDL levels were significantly greater in individuals with diabetes in any of the cohorts (Table 2), suggesting that lipoproteins do not contribute significantly to EV concentration.

To determine whether the onset of diabetes was associated with changes in EV concentration, we examined EV concentration in our longitudinal cohort (Fig. 1C). Participants who developed diabetes over the time period had elevated EV plasma concentration on average compared with the euglycemic group (Fig. 2F). The group that had

prediabetes and developed diabetes had the highest EV concentration over time compared with control subjects ( $P = 0.01$ ). There were no significant changes in EV size between individuals with diabetes and euglycemic individuals.

To further confirm our results obtained using precipitation isolation methods, we used a protocol recently reported by Kowal et al. (18) to compare EVs recovered from different steps of the differential ultracentrifugation protocol. Individuals with diabetes had higher concentration of EVs isolated at both medium (10,000g) and ultracentrifugation (120,000g) speeds (Fig. 2G). Thus, diabetes status is associated with higher levels of circulating EVs that include both classically defined exosomes and microvesicles according to isolation procedure.

Since plasma EVs are a heterogeneous population and little is known about the cell origin of plasma EVs, we wanted to determine whether diabetes results in higher levels of EVs derived from specific cells. To do this, we developed an antibody-based assay to compare cell-specific marker expression on the surface of intact EVs. We found that individuals with diabetes have significantly higher levels of CD235a-positive (erythrocyte) EVs and a trend toward higher CD68-positive (leukocytes) and CD62p-positive (platelet/endothelial cells) EVs (Fig. 2H). Levels of CD146-positive EVs (endothelial cells) were comparable between the two groups.

### Diabetes Alters Insulin Signaling Proteins in EVs

We used ELISAs to measure proteins from lysed EVs. We identified 12 proteins (phospho-p70S6K [Thr<sup>389</sup>], phospho-S6RP [Ser<sup>240/244</sup>], phospho-GSK3 $\beta$  [Ser<sup>9</sup>], phospho-AKT [Ser<sup>473</sup>], phospho-insulin receptor [IR] [Tyr], phospho-IRS1 [Ser<sup>312</sup>], tyr-phospho-IRS1, phospho-IGF-1R [Tyr], leptin receptor, and FGF21) involved in cellular insulin signaling in EVs. Leptin receptor and phospho-IR levels were decreased in EVs of individuals with diabetes (Fig. 3A).

Next, we examined the relationship between EV proteins and HOMA in this cohort. HOMA-B and HOMA-IR quantitatively measure  $\beta$ -cell function and insulin resistance, respectively. Linear mixed-model regression revealed that HOMA-B and HOMA-IR were significantly associated with EV concentration and with various insulin signaling proteins found in EVs (Fig. 3B). Examination of cross-sectional changes at time 2 revealed that higher HOMA-B levels were significantly associated with lower levels of phospho-S6RP, phospho-GSK3 $\beta$ , and phospho-AKT in EVs. Higher HOMA-IR was associated with lower phospho-S6RP in the cross-sectional analysis and higher FGF21 levels in the longitudinal and cross-sectional analyses (Fig. 3B). This indicates that EV cargo is affected by the different components of diabetes and may reflect the nature of the disease.

### Insulin Resistance Increases EV Secretion

Higher levels of circulating EVs in individuals with diabetes can be a consequence of several pathological causes. We wanted to test whether insulin resistance was related to

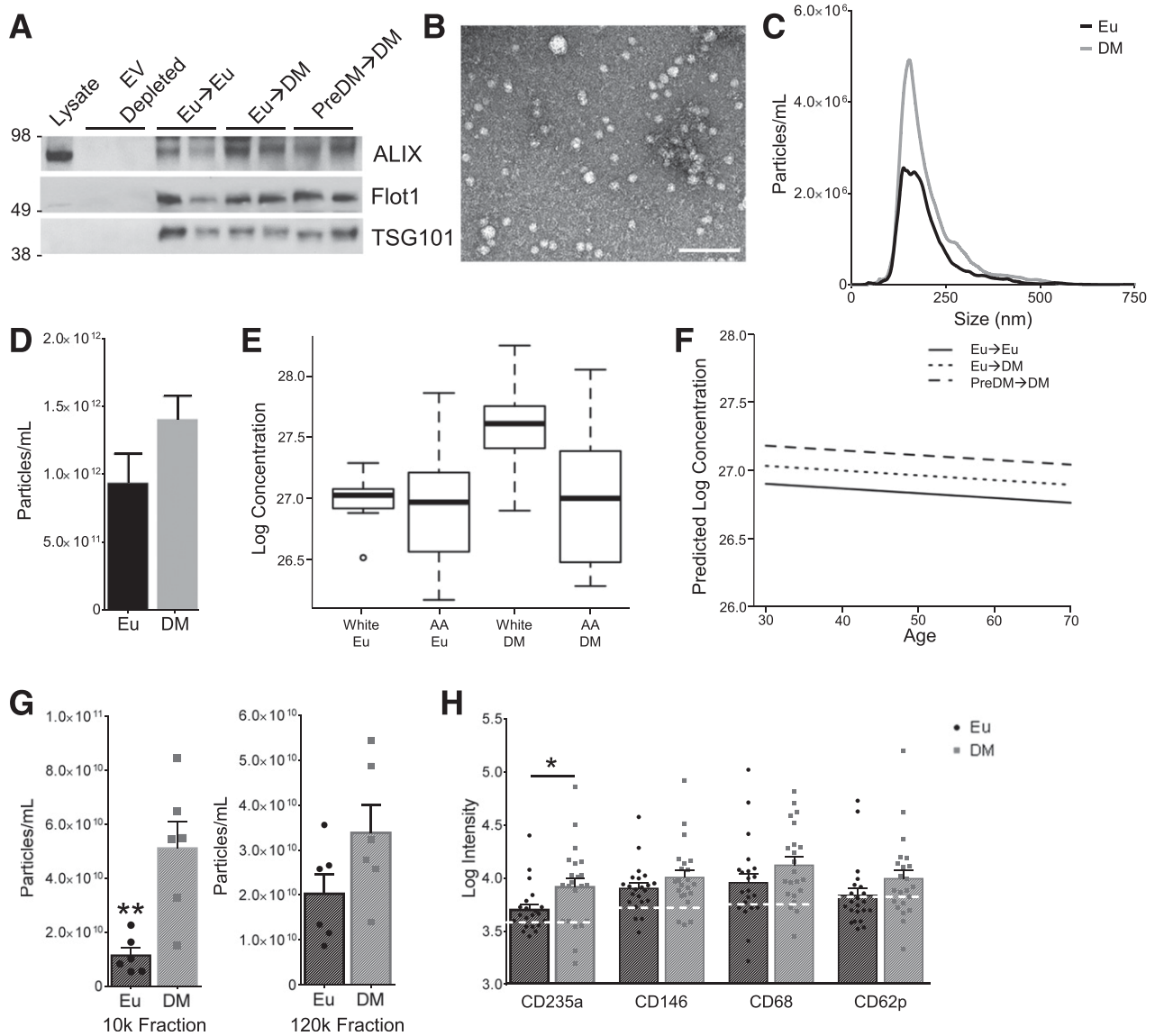


**Figure 2**—Higher plasma EV concentration in individuals with diabetes. **A**: Plasma-derived EVs isolated from six individuals (two from each longitudinal group), two EV-depleted plasma samples, and cell lysate from 3T3-L1 cells were subjected to SDS-PAGE and probed for EV-enriched proteins. **B**: Electron microscopy of EVs isolated from plasma exhibit expected morphology and size. Scale bar = 500 nm. **C** and **D**: EVs were isolated from the cross-sectional diabetes cohort and concentration and size distribution were analyzed using NTA. Size distribution was averaged for each group. The area under the curve in **C** is shown in **D**.  $P < 0.022$  by linear mixed-model regression. **E**: EV concentration for cross-sectional cohort 2.  $P < 0.016$  between white euglycemic individuals (Eu) and individuals with diabetes (DM) by linear mixed-model regression. AA, African American. **F**: EV concentration in a longitudinal cohort showed a significant difference between the euglycemic→euglycemic and prediabetes→diabetes groups ( $P = 0.01$ ) (DM, individuals with diabetes; PreDM, individuals with prediabetes). The histogram in **D** and line in **F** represent the predicted value from linear mixed-model regression.  $P$  value was determined by linear mixed-model regression on log-transformed values. **G**: NTA analysis of plasma EVs isolated from euglycemic individuals ( $n = 6$ ) and individuals with diabetes ( $n = 6$ ) from cross-sectional cohort 1 using differential ultracentrifugation. EVs were isolated from both the 10,000g and 120,000g fractions as indicated (\*\* $P < 0.01$ ). **H**: Antibodies against the cell-specific markers were used to capture intact euglycemic and diabetic ( $n = 22$ /group) PKH-labeled EVs from the cross-sectional cohort 2. Fluorescent intensity was measured, and log-transformed values are shown. Dashed white line indicates average IgG signal ( $n = 3$ ) for each assay. \* $P < 0.05$  by Student *t* test.

this increase in circulating EVs. We chose to use primary neuronal cells as a model because accumulating evidence links insulin resistance in the brain to neurodegenerative disorders including Parkinson and Alzheimer diseases (23,24). Moreover, little is known about the underlying factors that contribute to neuronal insulin resistance. AKT signaling was increased by acute insulin treatment (30 min)

(Fig. 4A). Consistent with insulin resistance, neurons pre-treated for 48 h with insulin and then treated with an acute insulin treatment had reduced capability to activate AKT signaling (Fig. 4A).

To examine the effects of prolonged insulin exposure on EV secretion from cortical neurons, we collected conditioned media after 30 min from each of the treatment

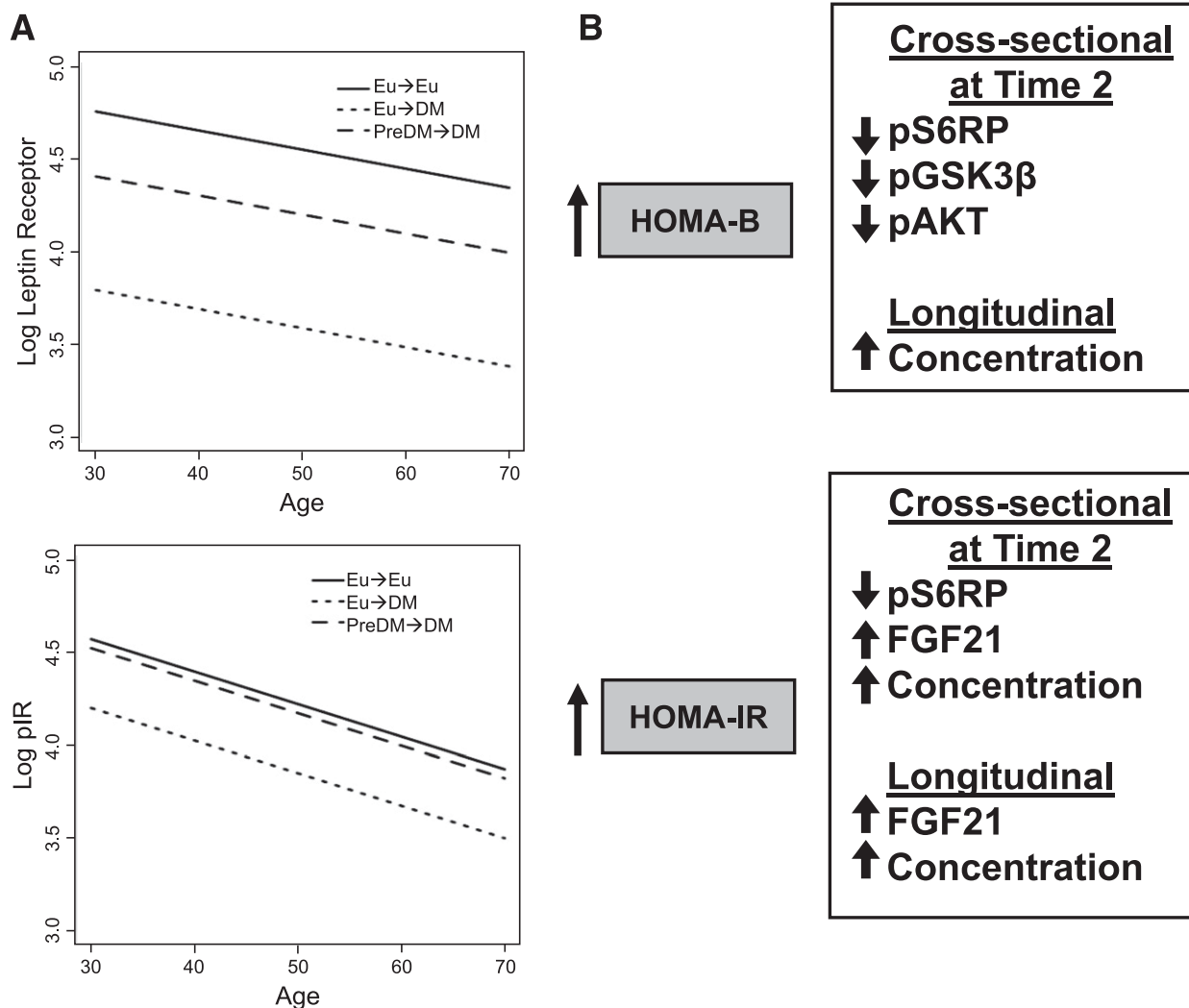


**Figure 3**—Insulin signaling proteins are present in EVs and are affected by diabetes status. *A*: EV protein levels of the leptin receptor and phosphorylated (p)IR were measured using ELISAs, and the lines represent the predicted values from linear mixed-model regression.  $P = 0.01$  for leptin receptor and  $P = 0.051$  for phospho-IR for euglycemia→euglycemia group ( $n = 19$ ) compared with the euglycemia→diabetes ( $n = 19$ ) group (DM, diabetes; Eu, euglycemic; PreDM, prediabetes). *B*: EV protein levels and concentration were quantified in the longitudinal cohort at both times (euglycemia→euglycemia,  $n = 19$ , and euglycemia→diabetes,  $n = 19$ ). A cross-sectional analysis was performed using time 2 (euglycemia = 19 and diabetes = 39). The relationship with HOMA-B and HOMA-IR was analyzed using linear mixed-model regression. Significant changes are indicated, and the direction of change is indicated by the up and down arrows.

groups. EVs were isolated and purity was assessed by immunoblotting for known EV markers as well as a negative control, Calnexin (Fig. 4B). NTA of EVs showed a peak around 140 nm (Fig. 4C). EV concentration was significantly higher in the media collected from cells exposed to insulin for 48 h and then treated with an acute insulin treatment (Fig. 4D). Insulin treatment for 48 h alone did not alter EV concentration (Fig. 4D). Insulin signaling protein levels were not significantly altered in the neuronal EVs after chronic or acute exposure to insulin (Supplementary Fig. 1). To exclude the effects of apoptotic bodies in the media, we assessed cell viability under different treatment conditions and found no significant differences (Supplementary Fig. 2). Collectively, these data indicate

that hyperinsulinemia induces insulin resistance in cortical neurons, leading to increased EV secretion.

Given that autophagy may play a role in neuronal insulin signaling in response to hyperinsulinemia (25), we treated insulin resistant primary cortical neurons with wortmannin, as it is a phosphatidylinositol 3-kinase/AKT class III inhibitor and other autophagy inhibitors can increase autophagy under nutrient-stressed conditions (26). Cells exposed to hyperinsulinemic conditions for 24 h showed higher levels of the autophagy marker LC3 II than untreated cells, and this was attenuated by treatment with wortmannin (Fig. 4E). Wortmannin significantly decreased EV secretion in insulin resistant neurons under these conditions (Fig. 4F), suggesting that

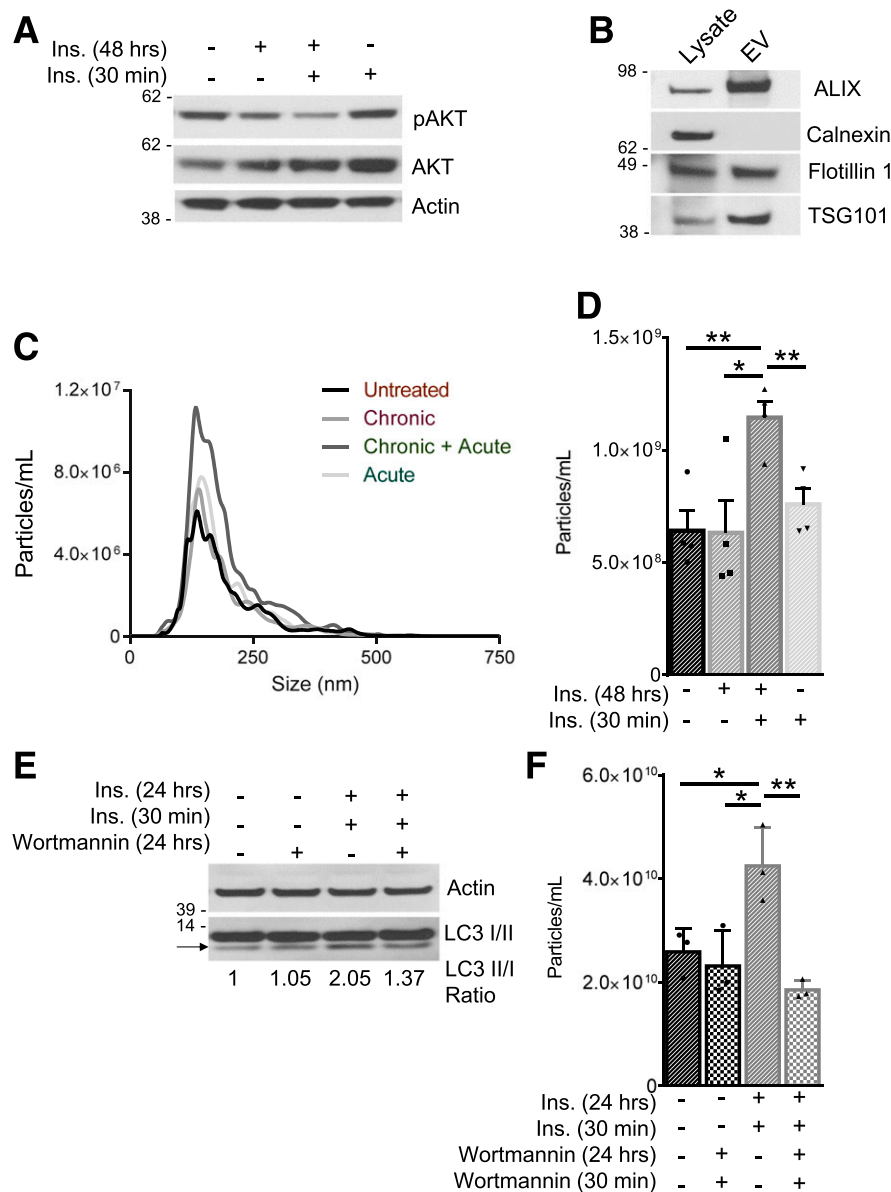


**Figure 4**—Prolonged exposure to insulin impairs insulin signaling in primary cortical neurons and increases EV secretion. Neurons were untreated, pretreated with insulin (Ins.) (200 nmol/L) for 48 h, and then either untreated or treated for 30 min with insulin (200 nmol/L) or treated only for 30 min with insulin as indicated. **A**: Neurons were lysed and immunoblotted with anti-phosphorylated (p)AKT, total AKT, or actin antibodies. **B**: The conditioned media was collected from treated neurons, and the EVs were isolated by differential ultracentrifugation. EVs were lysed and analyzed by SDS-PAGE along with cell lysate from primary cortical neurons. Samples were probed using antibodies for positive and negative EV markers. **C** and **D**: NTA was used to analyze the size distribution and concentration of EVs isolated from conditioned media from treated and untreated neurons ( $n = 4$ ). **E**: Neurons treated as described above were also incubated with 200 nmol/L wortmannin. Cell lysates were collected and immunoblotted with an anti-LC3 antibody. Arrow indicates LC3 II, and numbers indicate the ratio of LCII to LC I. Actin was used as a protein loading control. **F**: EVs were isolated from the conditioned media, and the concentration was measured using NTA ( $n = 3$ ). All histograms represent the mean (SEM). \*\* $P < 0.01$ , \* $P < 0.05$  by Student  $t$  test.

autophagy may be important for the increased neuronal EV secretion in response to insulin resistance.

#### EVs From Individuals With Diabetes Are Preferentially Internalized by Circulating Leukocytes

Diabetes is often associated with a heightened immune response; thus, we wanted to explore whether EVs contributed to this pathology. Previously, we developed a FACS-based

method to quantify EV internalization in cells that interact with circulating EVs: monocytes and B cells (17). Here, we chose to use this method to identify whether EVs from euglycemic individuals or individuals with diabetes are differentially internalized by leukocytes and alter signaling pathways. Monocytes (defined as classical [CD14<sup>++</sup>CD16<sup>-</sup>PKH<sup>+</sup>], nonclassical [CD14<sup>-</sup>CD16<sup>+</sup>PKH<sup>+</sup>], and intermediate [CD14<sup>++</sup>CD16<sup>+</sup>PKH<sup>+</sup>]) and B cells (CD19<sup>+</sup>PKH<sup>+</sup>)

internalized EVs from individuals with diabetes more readily than EVs from euglycemic individuals (Fig. 5 and Supplementary Figs. 3–6). EVs from individuals with diabetes did not significantly alter the surface levels of activation markers for B cells (CD25, CD80, MHC-II) and monocytes (MHC-II, CD80) (Supplementary Figs. 4–7).

To test whether other inflammatory signals are altered by internalization of diabetic EVs, we isolated RNA from monocytes incubated with EVs from euglycemic individuals or individuals with diabetes. Cells not treated with EVs were also used as an additional control. We performed a genome-wide microarray to assess gene expression changes and analyzed biological pathways. All significant pathways are included in Supplementary Fig. 8, while we focused primarily on pathways related to cell survival,

oxidative stress, and immune functions, as these occupy critical niches in type 2 diabetes (Fig. 6A). EVs from participants with diabetes increased genes that are related to immune function and inflammation (Fig. 6A). Apoptosis (*CRADD*, *DDIT3*, *BBC3*, and *DEDD2*) and oxidative stress pathways and genes (*GSTP1*, *SOD2*, *NCF1*, and *PARK7*) were downregulated in monocytes exposed to diabetic EVs (Fig. 6A and B).

To validate these results, we analyzed monocyte expression of selected genes by RT-qPCR. To confirm changes in inflammatory pathways, we collected the media and EVs from monocytes. Incubation of monocytes with EVs from individuals with diabetes decreased expression of apoptosis and oxidative stress-related genes and increased the levels of several cytokines in the media and in the EVs (Fig. 6C and D). Overall, these data indicate that EVs are internalized and affect signaling pathways in circulating leukocytes.

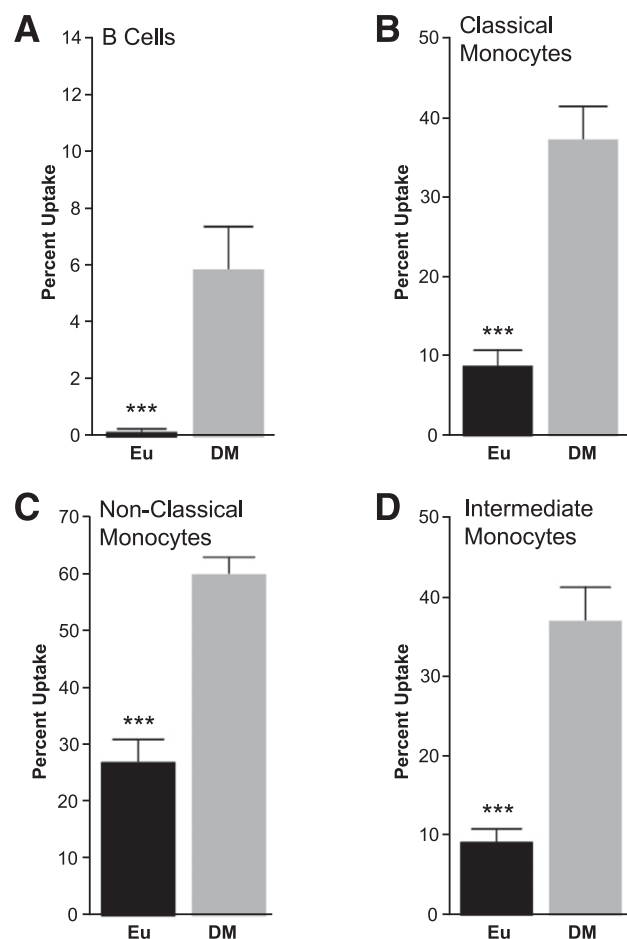


**Figure 5**—EVs from individuals with diabetes are preferentially internalized by circulating leukocytes. **A:** Plasma EVs ( $6 \times 10^8$ ) from individuals with diabetes ( $n = 39$ ) and euglycemic individuals ( $n = 19$ ) from the longitudinal cohort at time 2 were incubated with PBMCs ( $\sim 200,000$  cells/well) for 24 h. Cells positive for EV internalization (PKH<sup>+</sup>) were sorted into B cells (CD19<sup>+</sup>PKH<sup>+</sup>). **B:** Classical monocytes (CD14<sup>+</sup>CD16<sup>-</sup>PKH<sup>+</sup>). **C:** Nonclassical monocytes (CD14<sup>-</sup>CD16<sup>+</sup>PKH<sup>+</sup>). **D:** Intermediate monocytes (CD14<sup>+</sup>CD16<sup>+</sup>PKH<sup>+</sup>). The histograms represent means (SEM). Statistical significance was assessed by linear mixed-model regression on the log-transformed values to account for skewness of the data. DM, diabetes; Eu, euglycemic. \*\*\* $P < 0.001$ .

## DISCUSSION

Several studies have characterized the role that EVs play in modulating insulin signaling in mouse models (6,7,27) and in vitro studies (9,10,28); however, few studies examine EVs in type 2 diabetes using human cohorts. Here, we report differences in EV concentration, cargo, and function in three cohorts of individuals with diabetes and euglycemic individuals.

In our cross-sectional analyses, we observed higher levels of plasma EVs from individuals with diabetes compared with euglycemic control subjects. Longitudinally, individuals who were diagnosed with prediabetes during visit 1 and developed diabetes by visit 2 had a greater plasma EV concentration than participants who were euglycemic at both visits. These data corroborate previously reported findings that have shown that individuals with diabetes have higher levels of endothelium-derived microparticles, a subset of large EVs with endothelium-specific markers, in the circulation than euglycemic control subjects (12–14). Importantly, our assay examining cell-specific markers indicate that individuals with diabetes have higher levels of circulating CD235a-positive EVs. A trend toward higher levels of CD68-positive and CD62p-positive EVs was also observed. These data enhance available information about the variety of cell types that contribute to EVs in the circulation and how these EVs change with diabetes.

In humans, we found that EV concentration was positively correlated with HOMA-IR, suggesting that insulin resistance in vivo may contribute to higher EV levels. To test these findings, we exposed primary neurons to hyperinsulinemic conditions. In response to prolonged exposure to insulin, cells developed reduced insulin signaling and increased EV secretion. These data indicate that insulin resistance contributes to the higher EV concentration associated with diabetes. We also found that autophagy may play a role in this pathway.

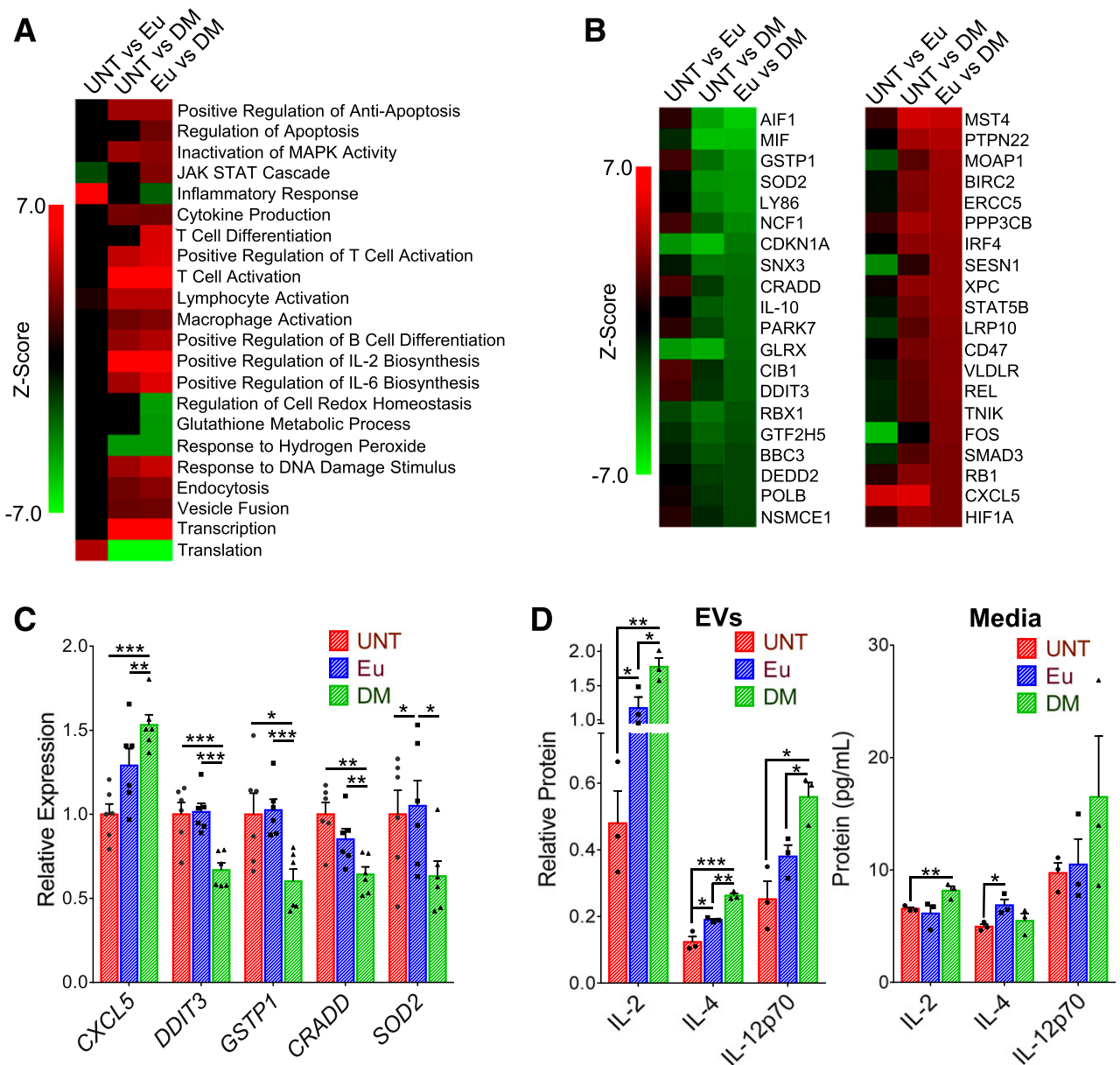


**Figure 6**—EVs from individuals with diabetes alter gene expression in monocytes. **A:** Plasma EVs were pooled ( $4.5 \times 10^{11}$ ) from several individuals from the longitudinal cohort at time 2 and grouped as either diabetic (DM) ( $n = 2$ ) or euglycemic (EU) ( $n = 3$ ). Cells not treated with EVs were used as another control (UNT). EVs were incubated with PBMCs for 24 h, and monocytes were isolated. Gene expression was assessed by microarray, and Gene Ontology analysis was performed. Heat map shows significant pathways ( $P < 0.01$ ) related to apoptosis, immune response, oxidative stress, and vesicle formation. **B:** Top 20 significant downregulated and upregulated genes from the pathways in **A** are shown. A  $P$  value cutoff of  $<0.05$  was used for significance. Labeling represents control group vs. treatment group. **C** and **D:** After incubation with euglycemic or diabetic EVs from cross-sectional cohort 2 ( $n = 3$ /group), total RNA and media were collected from the monocytes. Gene-specific primers were used for RT-qPCR analysis of genes from the microarray (**C**). **D:** EVs were isolated from the media using ultracentrifugation, lysed, and run along with EV-depleted media on a cytokine panel. Histograms represent the mean (SEM). \* $P \leq 0.05$ , \*\* $P < 0.01$ , \*\*\* $P < 0.001$  by Student  $t$  test.

EVs are readily internalized by cells (Supplementary Fig. 9) and elicit functional changes in target tissues and modulate insulin signaling in other tissues (6). Of the 12 insulin signaling proteins that we measured, the levels of the leptin receptor and phospho-IR were decreased longitudinally in EVs from participants who progressed from euglycemic to having diabetes compared with

euglycemic control subjects. It has been previously reported that diabetes status is positively correlated with levels of soluble insulin receptor in the blood (29). Although this may appear contradictory to the data reported here, it is difficult to know how changes in soluble insulin receptor relate to the changes in phospho-IR within EVs. Consistent with our data, an inverse correlation between soluble

leptin receptor levels and the risk of developing type 2 diabetes has previously been reported (30).

Phospho-AKT and phospho-GSK3 $\beta$  were negatively associated with HOMA-B, while phospho-S6RP was negatively associated with both HOMA-B and HOMA-IR in our cross-sectional analysis of time 2 (Fig. 3). Consistent with our findings in EVs, levels of activated proteins involved in AKT signaling are decreased in insulin resistant tissue (31). It is possible that the changes in proteins shuttled within EVs in the circulation directly reflect changes in the cells of origin in response to insulin resistance and  $\beta$ -cell function.

EVs from individuals with diabetes were preferentially internalized by monocytes and B cells compared with euglycemic individuals. Gene expression analysis showed that exposure to diabetic EVs resulted in upregulation of antiapoptotic genes in monocytes. As apoptosis regulation is a major factor in monocyte differentiation to dendritic cells (32), decreased apoptosis driven by diabetic EVs may result in increased monocyte differentiation.

Diabetic EVs also appeared to dampen processes related to oxidative stress response. Our data show a decrease in biological processes related to the regulation of cell redox homeostasis, glutathione metabolism, and response to hydrogen peroxide. Genes involved in oxidative stress management were decreased in our analysis. Low levels of the antioxidant SOD2 in monocytes have previously been shown in individuals with type 2 diabetes (33). These data suggest that internalization of EVs from individuals with diabetes inhibits oxidative stress response pathways in monocytes, which may affect phagocytosis function.

Previous studies have implicated EVs as a possible mediator of inflammation and immune cross talk in diabetic murine models (5) and insulin resistant tissue (10,28). Specifically, adipose-derived EVs from both mouse and human explants increased IL-6 production in macrophages (5,10). Here, we observed an increase in IL-2, IL-4, and IL-12p70 in EVs and IL-2 in the media from monocytes treated with EVs from individuals with diabetes. These data suggest that EVs from individuals with diabetes may affect inflammatory pathways.

These results demonstrate that EV concentration is higher in individuals with diabetes and EVs may be important signaling mediators in type 2 diabetes. Further defining the mechanism, we found that insulin resistance drives EV secretion. We have also shown alterations in the protein content of EVs that may serve as possible biomarkers for this chronic disease. EVs from individuals with diabetes are more readily internalized and affect monocyte function. Collectively, these data highlight the importance of EVs as diagnostic tools as well as mediators of type 2 diabetes.

---

**Acknowledgments.** The authors thank the HANDLS participants and the HANDLS medical staff. The authors thank Carol Cooke from the Johns Hopkins University Microscopy Core and Althaf Lohani from NIA for technical assistance.

The authors also thank NIA scientists Jennifer O'Connell and Calais Prince for critical reading of the manuscript and Dimitrios Kapogiannis for use of the NanoSight.

**Funding.** This study was supported by the NIA, NIH, Intramural Research Program (Inter-laboratory Funding [AG000989-01]).

**Duality of Interest.** No potential conflicts of interest relevant to this article were reported.

**Author Contributions.** D.W.F. and N.N.H. wrote the manuscript with input from all the authors. D.W.F., N.N.H., and E.E. conceived and designed the study with help from M.P.M. and M.K.E. D.W.F., N.N.H., E.E., and J.G. executed the experiments. J.E. provided consultation about insulin resistance experiments. N.A.M. and A.B.Z. performed statistical analysis. N.E. performed physical examination and interpreted laboratory analyses for all participants. M.B. performed PBMC EV internalization assay. Y.Z., E.L., and K.G.B. performed and analyzed gene expression microarrays. A.B.Z. and M.K.E. are co-principal investigators for HANDLS. Research was conducted in the laboratories of A.B., M.P.M., and M.K.E. M.K.E. is the guarantor of this work and, as such, had full access to all the data in the study and takes responsibility for the integrity of the data and the accuracy of the data analysis.

## References

1. Centers for Disease Control and Prevention. *National Diabetes Statistics Report 2017*. Atlanta, GA, U.S. Department of Health and Human Services, 2017
2. Banner K, Lichtenauer M, Franz M, et al. Impact of diabetes mellitus and its complications: survival and quality-of-life in critically ill patients. *J Diabetes Complications* 2015;29:1130–1135
3. Yáñez-Mó M, Siljander PR, Andreu Z, et al. Biological properties of extracellular vesicles and their physiological functions. *J Extracell Vesicles* 2015;4:27066
4. Perakis S, Speicher MR. Emerging concepts in liquid biopsies. *BMC Med* 2017;15:75
5. Deng ZB, Poliakov A, Hardy RW, et al. Adipose tissue exosome-like vesicles mediate activation of macrophage-induced insulin resistance. *Diabetes* 2009;58:2498–2505
6. Aswad H, Forterre A, Wiklander OP, et al. Exosomes participate in the alteration of muscle homeostasis during lipid-induced insulin resistance in mice. *Diabetologia* 2014;57:2155–2164
7. Jalabert A, Vial G, Guay C, et al. Exosome-like vesicles released from lipid-induced insulin-resistant muscles modulate gene expression and proliferation of beta recipient cells in mice. *Diabetologia* 2016;59:1049–1058
8. Ying W, Riopel M, Bandyopadhyay G, et al. Adipose tissue macrophage-derived exosomal miRNAs can modulate in vivo and in vitro insulin sensitivity. *Cell* 2017;171:372–384.e12
9. Kranendonk ME, Visseren FL, van Herwaarden JA, et al. Effect of extracellular vesicles of human adipose tissue on insulin signaling in liver and muscle cells. *Obesity (Silver Spring)* 2014;22:2216–2223
10. Kranendonk ME, Visseren FL, van Balkom BW, et al. Human adipocyte extracellular vesicles in reciprocal signaling between adipocytes and macrophages. *Obesity (Silver Spring)* 2014;22:1296–1308
11. Agouni A, Lagrue-Lak-Hal AH, Ducluzeau PH, et al. Endothelial dysfunction caused by circulating microparticles from patients with metabolic syndrome. *Am J Pathol* 2008;173:1210–1219
12. Esposito K, Maiorino MI, Di Palo C, et al. Effects of pioglitazone versus metformin on circulating endothelial microparticles and progenitor cells in patients with newly diagnosed type 2 diabetes—a randomized controlled trial. *Diabetes Obes Metab* 2011;13:439–445
13. Feng B, Chen Y, Luo Y, Chen M, Li X, Ni Y. Circulating level of microparticles and their correlation with arterial elasticity and endothelium-dependent dilation in patients with type 2 diabetes mellitus. *Atherosclerosis* 2010;208:264–269
14. Li S, Wei J, Zhang C, et al. Cell-derived microparticles in patients with type 2 diabetes mellitus: a systematic review and meta-analysis. *Cell Physiol Biochem* 2016;39:2439–2450

15. Hromada C, Mühleder S, Grillari J, Redl H, Holnthoner W. Endothelial extracellular vesicles—promises and challenges. *Front Physiol* 2017;8:275
16. Matthews DR, Hosker JP, Rudenski AS, Naylor BA, Treacher DF, Turner RC. Homeostasis model assessment: insulin resistance and beta-cell function from fasting plasma glucose and insulin concentrations in man. *Diabetologia* 1985;28:412–419
17. Eitan E, Green J, Bodogai M, et al. Age-related changes in plasma extracellular vesicle characteristics and internalization by leukocytes. *Sci Rep* 2017;7:1342
18. Kowal J, Arras G, Colombo M, et al. Proteomic comparison defines novel markers to characterize heterogeneous populations of extracellular vesicle subtypes. *Proc Natl Acad Sci U S A* 2016;113:E968–E977
19. Zhang S, Eitan E, Wu T-Y, Mattson MP. Intercellular transfer of pathogenic  $\alpha$ -synuclein by extracellular vesicles is induced by the lipid peroxidation product 4-hydroxynonenal. *Neurobiol Aging* 2018;61:52–65
20. Noren Hooten N, Fitzpatrick M, Kompaniez K, et al. Coordination of DNA repair by NEIL1 and PARP-1: a possible link to aging. *Aging (Albany NY)* 2012;4:674–685
21. R Development Core Team. *R: A Language and Environment for Statistical Computing*. 3.3.2 ed. Vienna, Austria, R Foundation for Statistical Computing, 2010
22. Lötval J, Hill AF, Hochberg F, et al. Minimal experimental requirements for definition of extracellular vesicles and their functions: a position statement from the International Society for Extracellular Vesicles. *J Extracell Vesicles* 2014;3:26913
23. Schubert M, Gautam D, Surjo D, et al. Role for neuronal insulin resistance in neurodegenerative diseases. *Proc Natl Acad Sci U S A* 2004;101:3100–3105
24. Willette AA, Bendlin BB, Starks EJ, et al. Association of insulin resistance with cerebral glucose uptake in late middle-aged adults at risk for alzheimer disease. *JAMA Neurol* 2015;72:1013–1020
25. Mayer CM, Belsham DD. Central insulin signaling is attenuated by long-term insulin exposure via insulin receptor substrate-1 serine phosphorylation, proteasomal degradation, and lysosomal insulin receptor degradation. *Endocrinology* 2010;151:75–84
26. Wu YT, Tan HL, Shui G, et al. Dual role of 3-methyladenine in modulation of autophagy via different temporal patterns of inhibition on class I and III phosphoinositide 3-kinase. *J Biol Chem* 2010;285:10850–10861
27. Chen J, Chen S, Chen Y, et al. Circulating endothelial progenitor cells and cellular membrane microparticles in db/db diabetic mouse: possible implications in cerebral ischemic damage. *Am J Physiol Endocrinol Metab* 2011;301:E62–E71
28. Zhang Y, Shi L, Mei H, et al. Inflamed macrophage microvesicles induce insulin resistance in human adipocytes. *Nutr Metab (Lond)* 2015;12:21
29. Hiriart M, Sanchez-Soto C, Diaz-Garcia CM, et al. Hyperinsulinemia is associated with increased soluble insulin receptors release from hepatocytes. *Front Endocrinol (Lausanne)* 2014;5:95
30. Sun Q, van Dam RM, Meigs JB, Franco OH, Mantzoros CS, Hu FB. Leptin and soluble leptin receptor levels in plasma and risk of type 2 diabetes in U.S. women: a prospective study. *Diabetes* 2010;59:611–618
31. Kim B, Sullivan KA, Backus C, Feldman EL. Cortical neurons develop insulin resistance and blunted Akt signaling: a potential mechanism contributing to enhanced ischemic injury in diabetes. *Antioxid Redox Signal* 2011;14:1829–1839
32. Cheng DE, Chang WA, Hung JY, Huang MS, Kuo PL. Involvement of IL-10 and granulocyte colony-stimulating factor in the fate of monocytes controlled by galectin-1. *Mol Med Rep* 2014;10:2389–2394
33. Bauer S, Wanninger J, Neumeier M, et al. Elevated free fatty acids and impaired adiponectin bioactivity contribute to reduced SOD2 protein in monocytes of type 2 diabetes patients. *Exp Mol Pathol* 2011;90:101–106

SUPPLEMENTARY DATA

**Altered Extracellular Vesicle Concentration, Cargo and Function in Diabetes Mellitus**

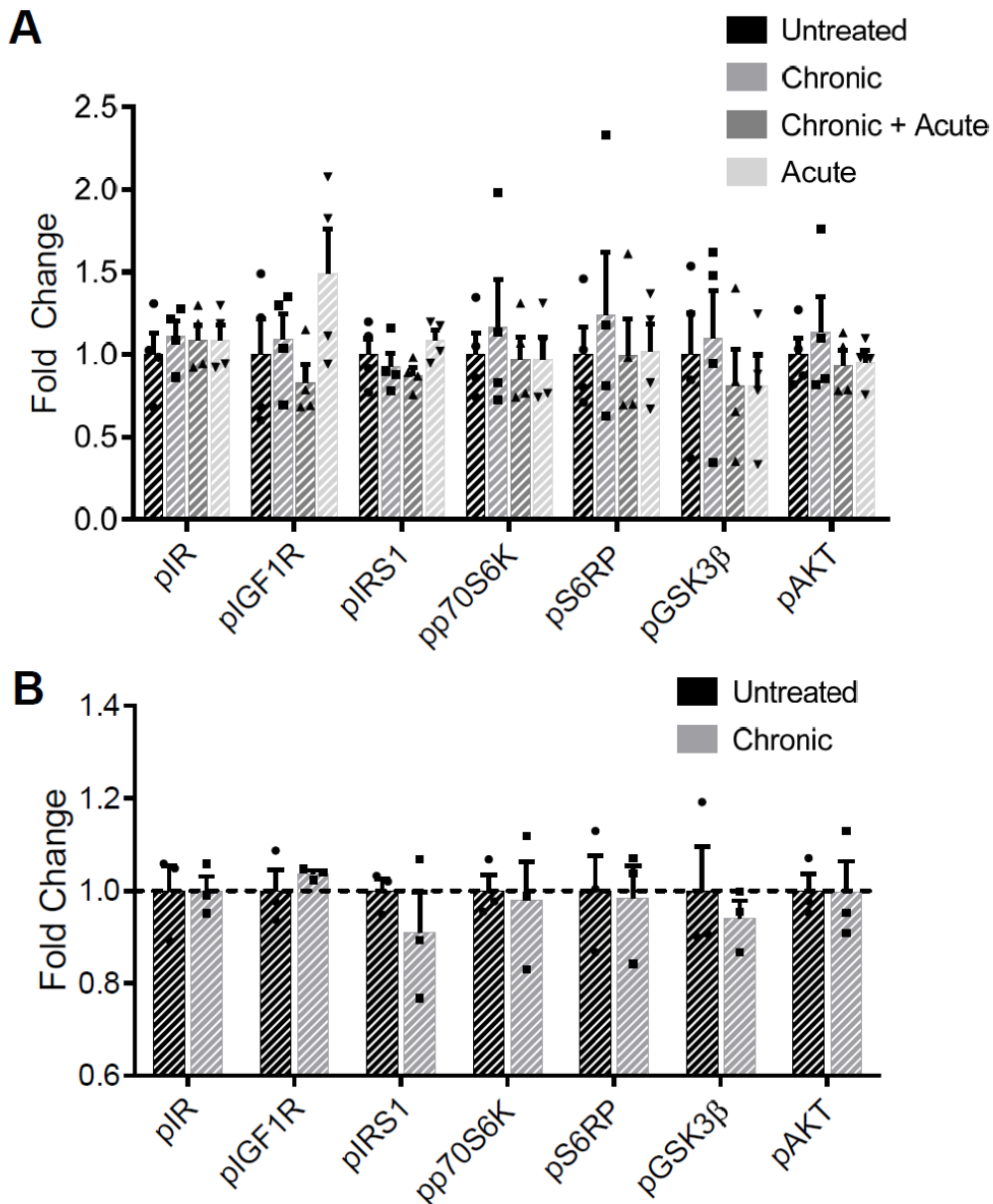
David W. Freeman, Nicole Noren Hooten, Erez Eitan, Jamal Green, Nicolle A. Mode, Monica Bodogai, Yongqing Zhang, Elin Lehrmann, Alan B. Zonderman, Arya Biragyn, Josephine Egan, Kevin G. Becker, Mark P. Mattson, Ngozi Ejiogu, and Michele K. Evans

**Supplementary Table S1. Primer sequences for RT-qPCR**

<b>CRADD</b>	GGGCAGGTTCCCTAACAGTCA	TACTTGTTTGTCTCTGGCCTCCAT
<b>CXCL5</b>	GGAGTTCATCCCAAATGATCAGT	CAAATTCCTTCCCGTTCTTCA
<b>DDIT3</b>	AGAACCAGGAAACGGAAACAGA	TCTCCTTCATGCGCTGCTTT
<b>GSTP1</b>	CCTGGTGGACATGGTGAATG	CCGCCTCATAGTTGGTGTAGATG
<b>HPRT</b>	AGATGGTCAAGGTCGCAAGCT	GGGCATATCCTACAACAACTTGTC
<b>SOD2</b>	GCCCTGGAACCTCACATCAA	CCAACGCCTCCTGGTACTTC
<b>UBC</b>	ATTTGGGTCGCGGTTCTTG	TGCCTTGACATTCTCGATGGT

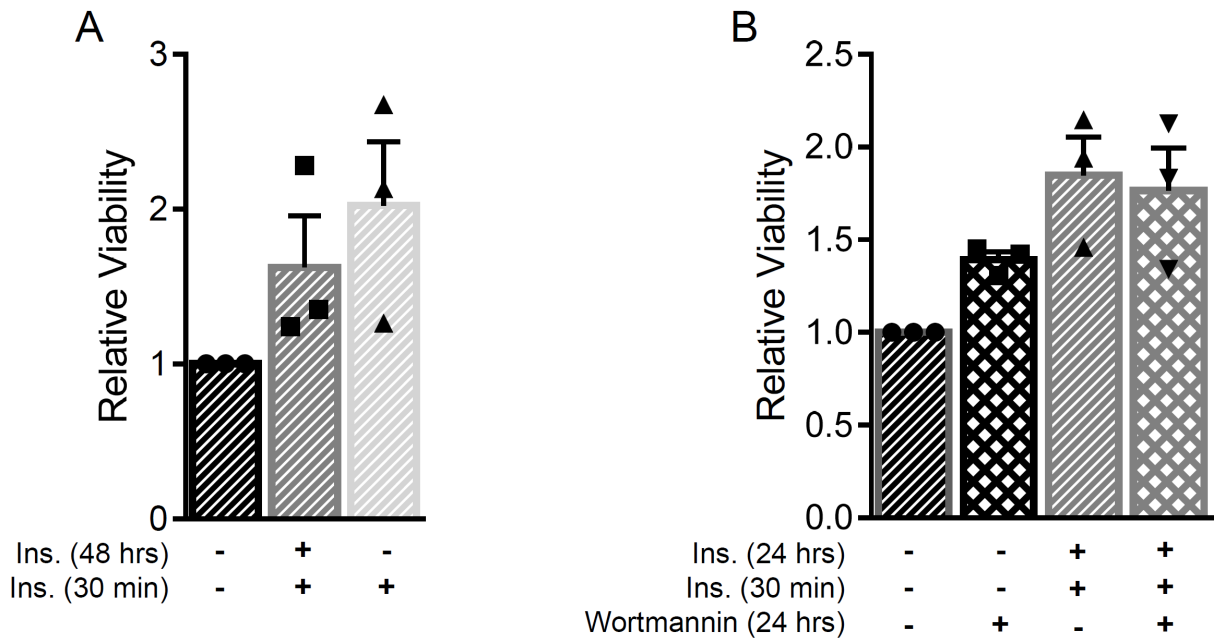
SUPPLEMENTARY DATA

**Supplementary Figure S1.** EV neuronal cargo after insulin treatment. **(A)** EVs were isolated from primary cortical neurons treated with either no insulin (untreated), insulin for 48 hours (chronic), insulin for 48 hours followed by 30 minutes with fresh insulin (chronic + acute) or no insulin for 48 hours followed by 30 minutes with fresh insulin (acute). **(B)** Primary cortical neurons were incubated with fresh media for 48 hours either containing no insulin (untreated) or 200nM of insulin (chronic). The vesicles were lysed and protein content was analyzed using the AKT signaling panel II and insulin signaling kits from MesoScale Diagnostics. The histograms represent the mean + SEM (n=4 for A and n=3 for B).



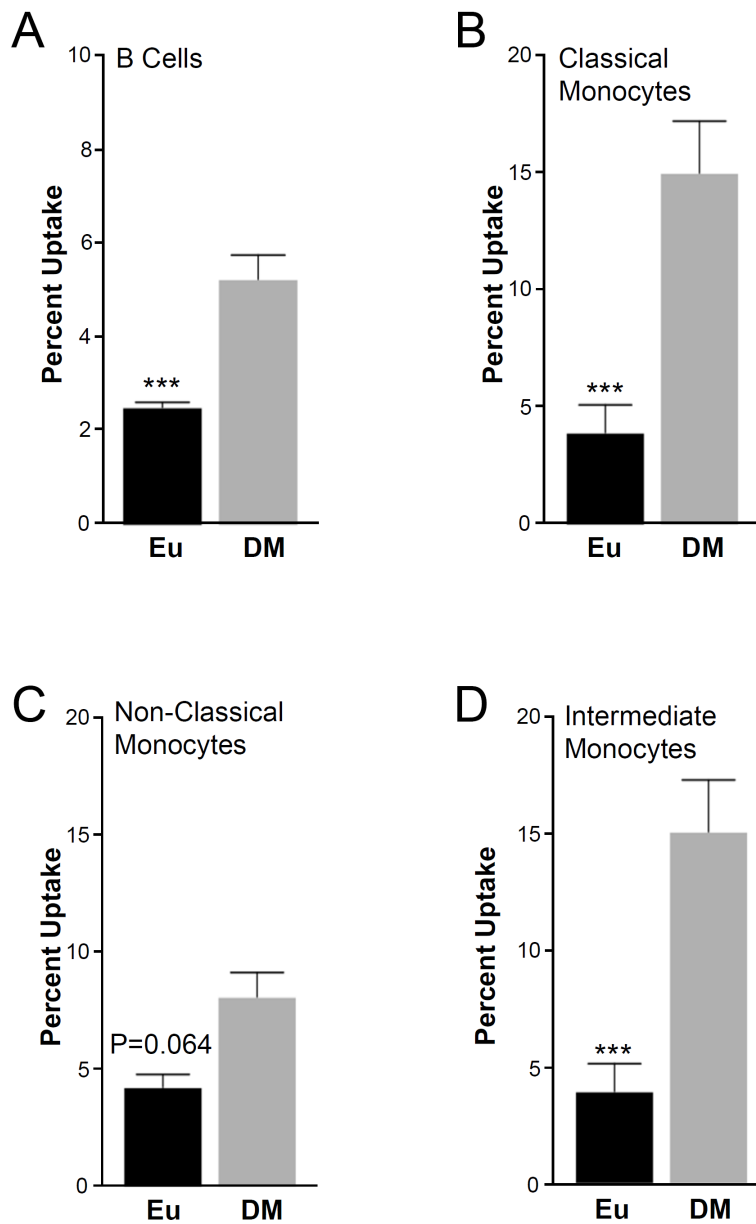
SUPPLEMENTARY DATA

**Supplementary Figure S2.** Cell viability of primary cortical neurons. **(A)** Primary cortical neurons were treated with insulin (200nM) for the indicated times. Cell viability was measured using a MTT assay. **(B)** Neurons were treated as in (A) in the absence or presence of wortmannin. Each experiment was performed in triplicate. The histogram represents the mean + SEM from 3 independent experiments.



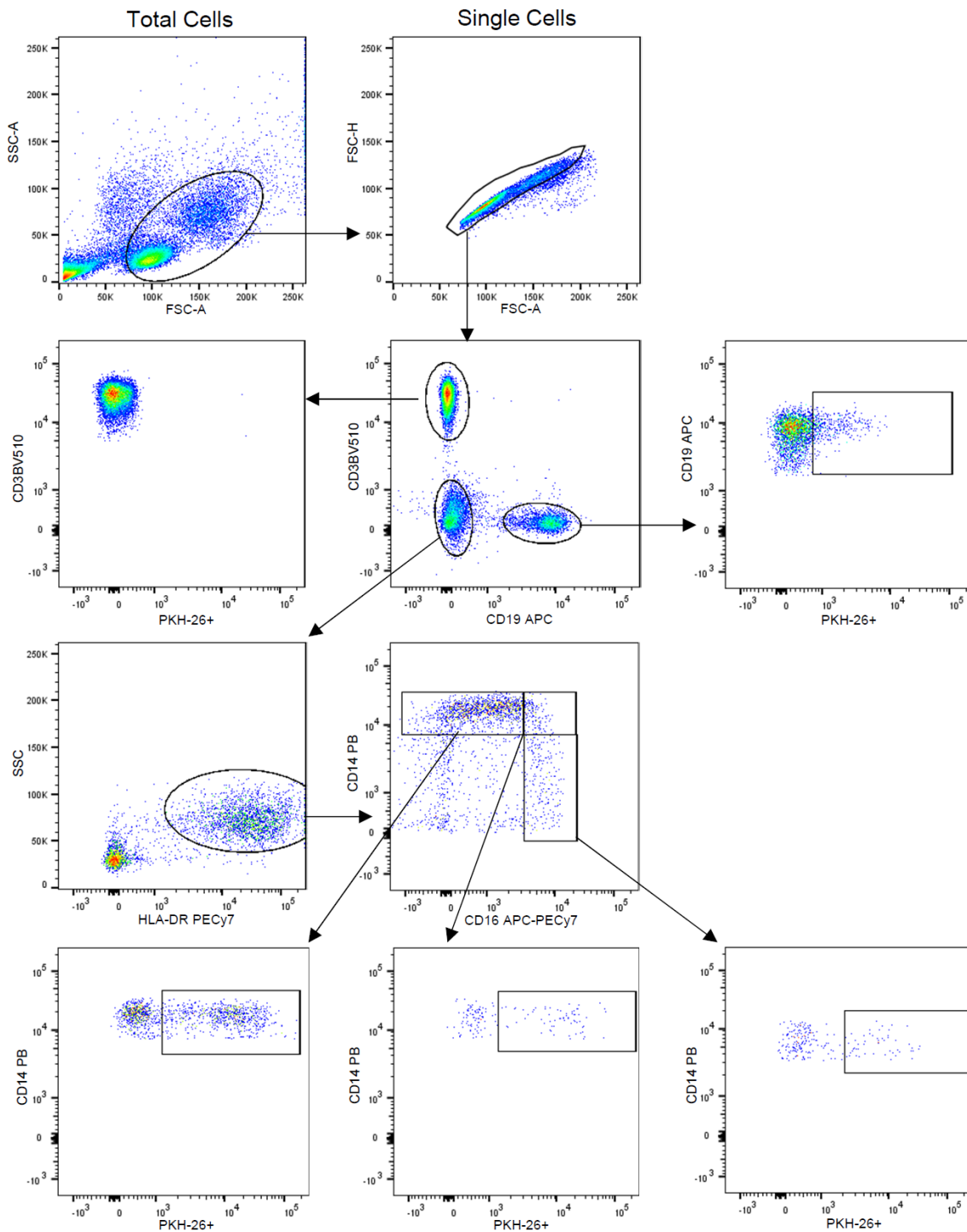
SUPPLEMENTARY DATA

**Supplementary Figure S3.** PBMC internalization of EVs from diabetic and euglycemic individuals. **(A)** PBMCs (~200,000 cells) were incubated with plasma EVs ( $3 \times 10^8$ ) from diabetic (DM, n=39) and euglycemic (Eu, n=19) for 24 hours. Cells were sorted by FACS into B cells that had internalized EVs ( $CD19^+PKH^+$ ) **(B)** classical monocytes that had internalized EVs ( $CD14^{++}CD16^-PKH^+$ ) **(C)** non-classical monocytes that had internalized EVs ( $CD14^+CD16^+PKH^+$ ) and **(D)** intermediate monocytes that had internalized EVs ( $CD14^{++}CD16^+PKH^+$ ). The histograms represent the mean + S.E.M. The data was log transformed and significance was calculated using linear mixed model regression taking into account matching. \*\*\* $P < 0.001$



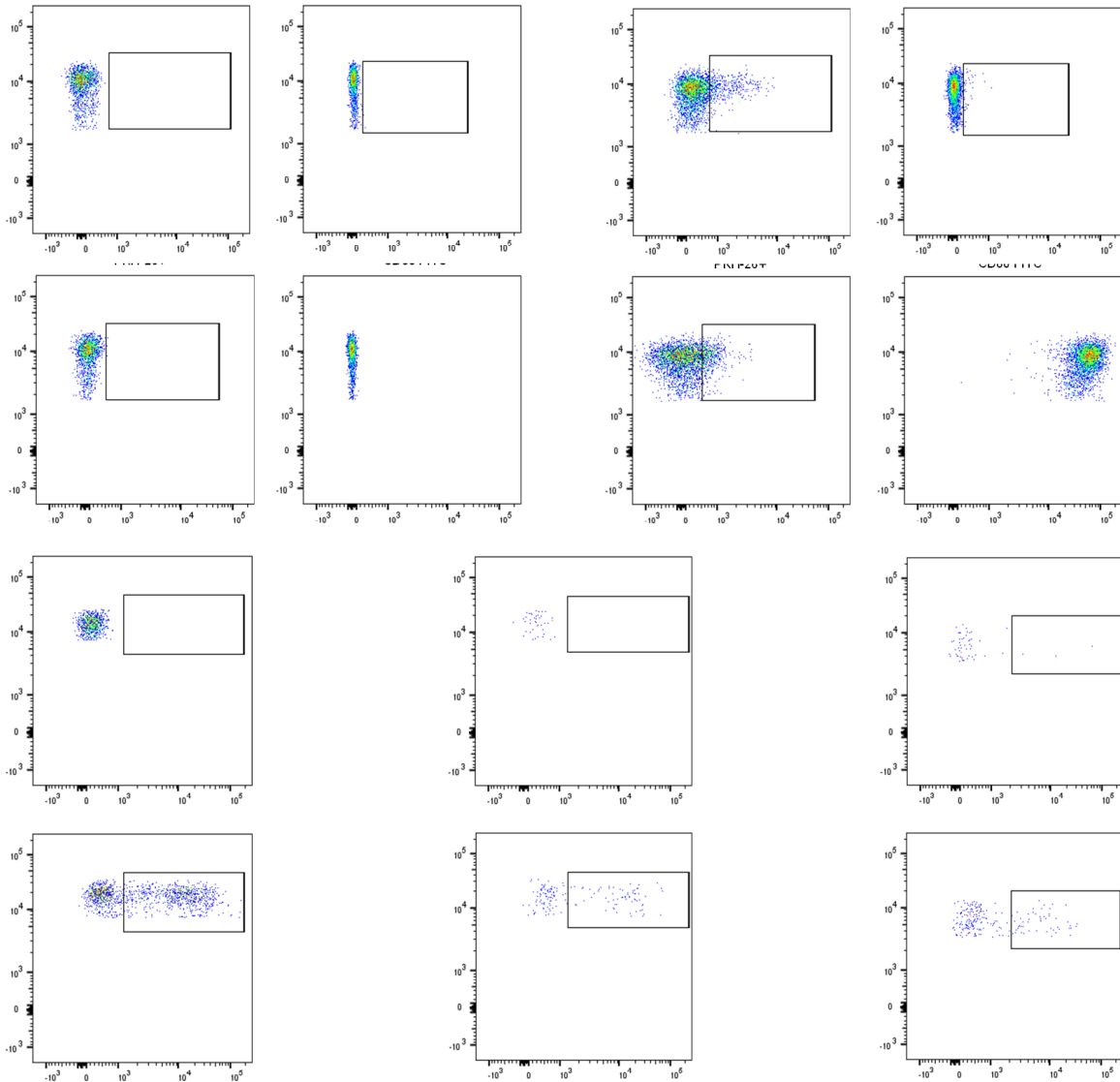
SUPPLEMENTARY DATA

**Supplementary Figure S4.** FACS gating for EV internalization assays. PBMCs were incubated with PKH26-labeled EVs as described in Research Design and Methods. Cells were sorted into PKH+ and PKH- T Cells (CD3<sup>+</sup>), B Cells (CD19<sup>+</sup>), intermediate monocytes (CD14<sup>++</sup>CD16<sup>+</sup>), classical monocytes (CD14<sup>++</sup>CD16<sup>-</sup>) and nonclassical monocytes (CD14<sup>+</sup>CD16<sup>+</sup>PKH<sup>+</sup>). Representative FACS plots are shown.



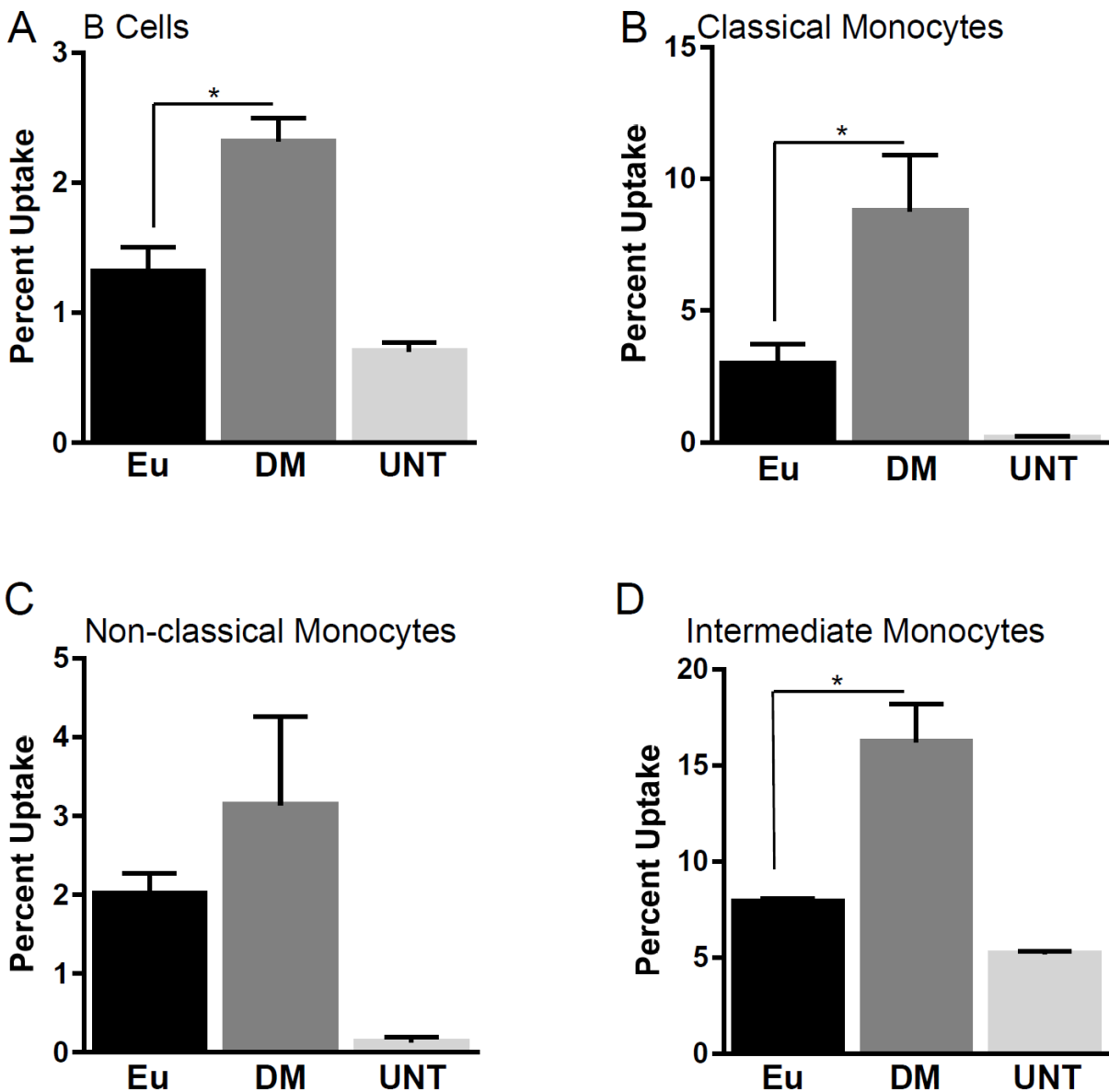
SUPPLEMENTARY DATA

**Supplementary Figure S5.** FACS sorting controls for EV internalization assay. **(A,B)** Representative FACS plots of B Cells ( $CD19^+$ ) sorted for either PKH-26, CD80, CD25 or MHC-II are shown. Samples were stained for IgG control (A) or specific antibodies (B). **(C-E)** Representative FACS plots of monocytes ( $CD14^+$ ) sorted into (C) classical monocytes ( $CD14^{++}CD16^-$ ), (D) intermediate monocytes ( $CD14^{++}CD16^+$ ) or (E) non-classical monocytes ( $CD14^+CD16^+$ ). Cells were incubated with either PBS and stained with a CD14 isotype control or incubated with PKH-labeled EVs and stained with a Pacific Blue conjugated CD14 antibody as denoted on the plots.



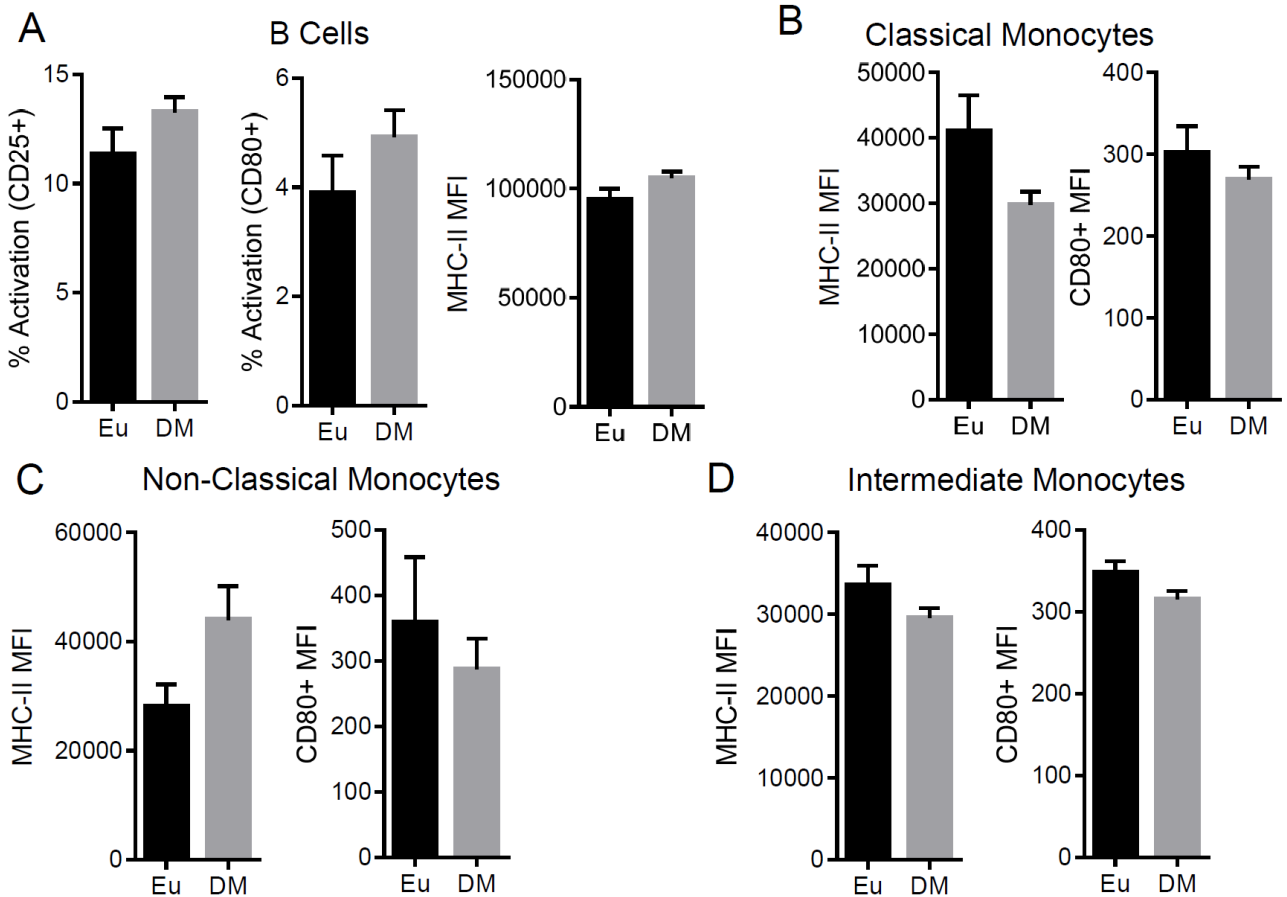
SUPPLEMENTARY DATA

**Supplementary Figure S6.** Monocyte internalization of diabetic and euglycemic EVs from the microarray experiment. **(A)** PKH26 labeled EVs from several individuals were pooled ( $4.5 \times 10^{11}$ ) and grouped as either diabetic (DM, n=3) or euglycemic (Eu, n=3) and incubated with PBMCs for 24 hours. PBS with PKH26 was used as a negative control (UNT, n=3). A small aliquot was taken for FACS analysis while RNA from the remaining cells was isolated and used for microarray. The FACS aliquot was sorted into B cells that had internalized EVs ( $CD19^+PKH^+$ ) **(B)** classical monocytes that had internalized EVs ( $CD14^{++}CD16^-PKH^+$ ) **(C)** non-classical monocytes that had internalized EVs ( $CD14^-CD16^+PKH^+$ ) and **(D)** intermediate monocytes that had internalized EVs ( $CD14^{++}CD16^+PKH^+$ ). Histograms represent the mean + SEM. Statistical significance was calculated using student's T test. \* $P < 0.05$ .



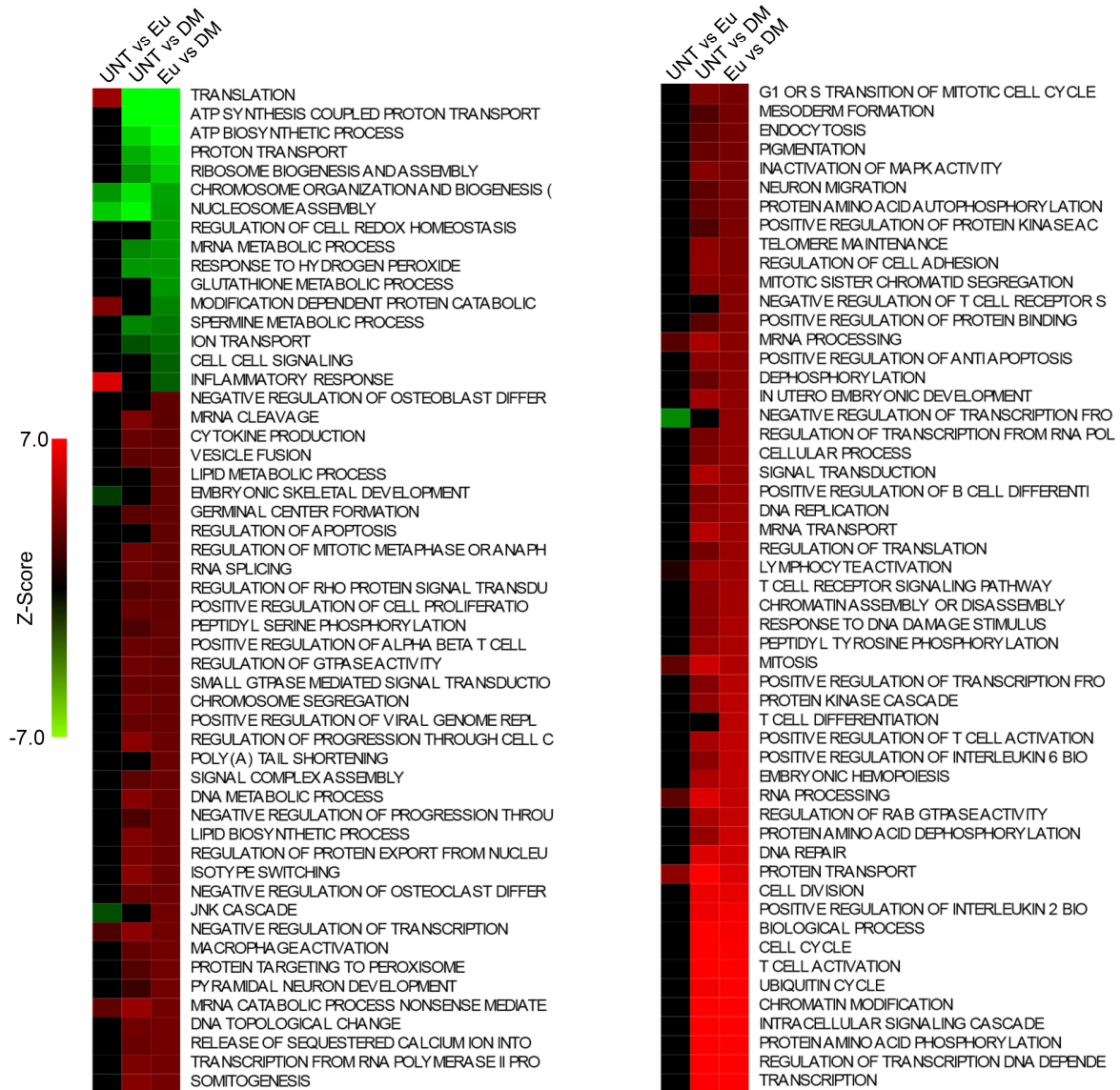
SUPPLEMENTARY DATA

**Supplementary Figure S7.** PBMC activation levels following EV internalization. PBMCs (~200,000 cells) were incubated with plasma EVs ( $3 \times 10^8$ ) from diabetic (DM, n=39) and euglycemic (Eu, n=19) for 24 hours and cells were sorted by FACS. **(A)** B cells that had internalized EVs expressing either CD25 (CD19<sup>+</sup>PKH<sup>+</sup>CD25<sup>+</sup>), CD80 (CD19<sup>+</sup>PKH<sup>+</sup>CD80<sup>+</sup>) or MHC-II (CD19<sup>+</sup>PKH<sup>+</sup>MHC-II<sup>+</sup>). **(B-D)** Monocytes were subdivided into either (B) classical monocytes that had internalized EVs (CD14<sup>++</sup>CD16<sup>-</sup>PKH<sup>+</sup>CD25<sup>+</sup>) (C) non-classical monocytes that had internalized EVs (CD14<sup>-</sup>CD16<sup>+</sup>PKH<sup>+</sup>) and (D) intermediate monocytes that had internalized EVs (CD14<sup>++</sup>CD16<sup>+</sup>PKH<sup>+</sup>) and the mean fluorescent intensity (MFI) for MHC-II and CD80 were measured.



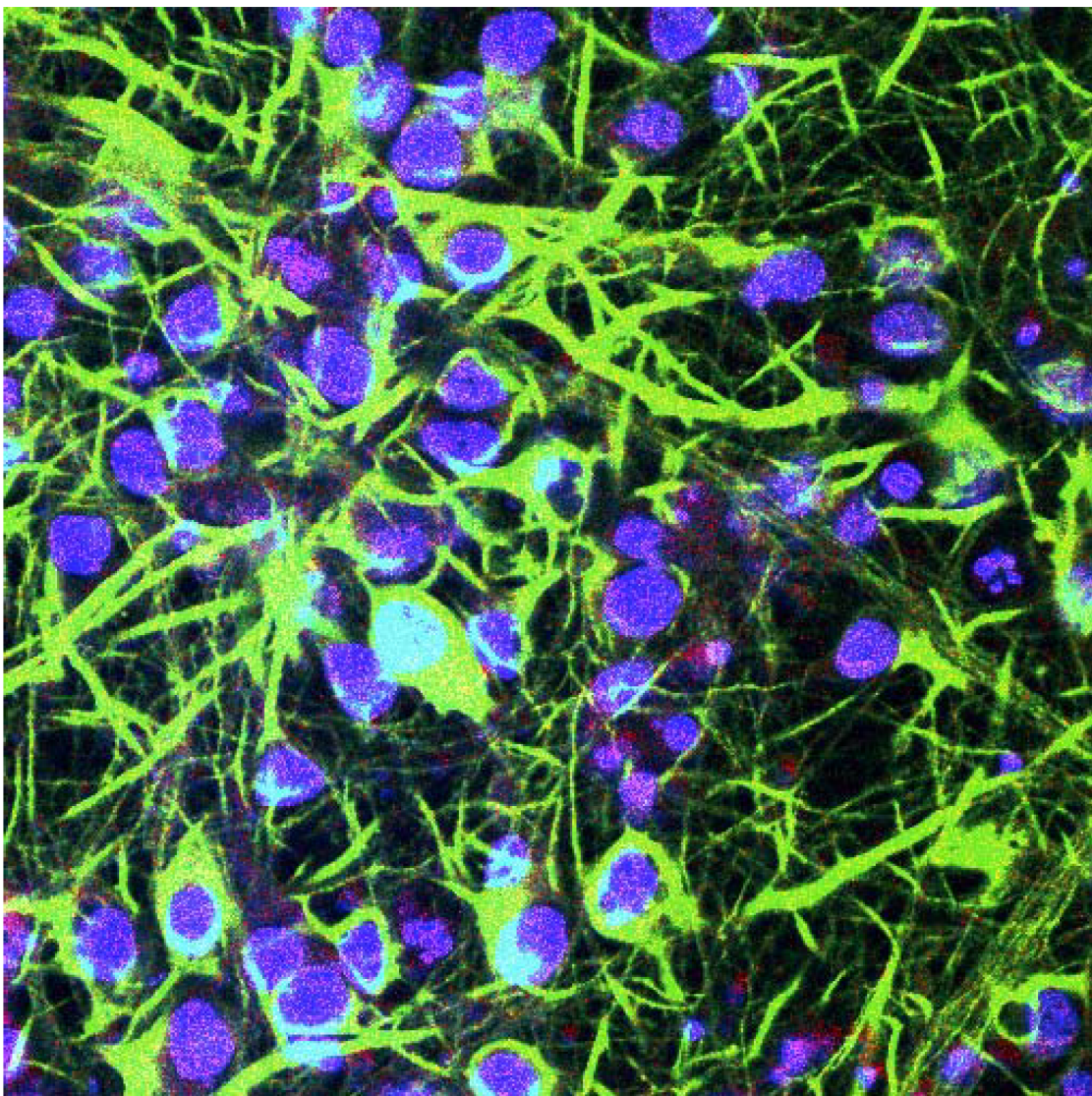
SUPPLEMENTARY DATA

**Supplementary Figure S8.** Significant biological pathways altered in monocytes by EVs from diabetic individuals. Plasma EVs ( $4.5 \times 10^{11}$ ) from diabetic (DM, n=2) or euglycemic (Eu, n=3) individuals were incubated with PBMCs for 24 hours or untreated (UNT). Monocytes were isolated using FACS and gene expression was assessed via microarray. Significant biological pathways ( $P < 0.01$ ) are visualized on the heat map.



## SUPPLEMENTARY DATA

**Supplementary Figure S9.** EVs are internalized by cells. Similar EV internalization assays were performed as we previously reported (Eitan E. et al., *NPJ Aging Mech.Dis.* 2016; Zhang, S. et al., *Neuro. Biol. of Aging* 2018). Primary cortical neurons were incubated with PKH26-labeled EVs in a ratio ~300 vesicles per neuron for 2 hours. Neurons were washed twice with PBS and fixed in 4% paraformaldehyde/PBS for 20 min. Fixed cells were incubated in blocking solution (0.3% Triton X-100 and 10% normal goat serum in PBS) for 30 min, and then incubated overnight at 4°C with antibodies against the neuronal marker MAP2 (Hm2, Sigma M9942). Cells were washed three times and incubated with Alexa Fluor 488 tagged anti-mouse secondary antibodies (Invitrogen) in blocking solution for 1 hr. The cells were then washed twice with PBS and nuclei were stained with DAPI (Sigma #32670). Coverslips were washed and mounted on slides in an anti-fade medium (Vector Laboratories, Burlingame, CA, USA). Images were acquired using a Zeiss LSM 510 confocal microscope with a 40 × objective. A representative confocal image of EV internalization is shown.





# Exosomes or Microvesicles, a Secreted Subcellular Organelle Contributing to Inflammation and Diabetes

Yang D. Dai<sup>1,2</sup> and Peter Dias<sup>1</sup>

*Diabetes* 2018;67:2154–2156 | <https://doi.org/10.2337/dbi18-0021>

Type 1 and type 2 diabetes (T1D and T2D) are generally recognized as distinct disease entities based on the mechanism of induction of disease: T1D results from low or no insulin production due to the gradual loss of cells that produce insulin, whereas T2D is generally thought to occur as a result of the body's development of resistance to insulin. Although the events initiating T1D and T2D might be very different, the progression to diabetes and complications are similar and involve interactions between the immune system and the metabolic system. Notably, chronic inflammation is a shared manifestation of the two types of diabetes (1,2). Recently, secreted microvesicles, particularly exosomes, were suggested to be intermediates linking inflammation to diabetes (3). The cellular origins of the vesicles and the genetic and environmental factors that cause an abnormal production of the vesicles are likely to be central in linking the inflammation to tissue-specific damage. For example, islet mesenchymal stem cells from autoimmune-prone animals were shown to release highly proinflammatory exosomes that contributed to T1D (4), and the low-grade inflammation in obesity may stimulate release of proinflammatory microvesicles and exosomes to accelerate T2D (5,6).

“Extracellular vesicles” (EVs) is a collective term for different types of small-sized membrane vesicles or particles that are secreted by cells, including exosomes, microvesicles, apoptotic bodies, and virus-like particles. Figure 1 shows a generalization of their similarities and differences in biogenesis and immune-stimulatory function. There are many reasons that such organelles may be produced, including packaging of paracrine factors for intercellular communications, apoptosis resulting from breakdown of cells, and packaging of material for ingestion and disposal by scavenger cells (7). Viruses too have learned to take advantage of the vesicle biogenesis machinery to hide from immune surveillance to establish infections at immune-privileged sites (8,9). Therefore, EV preparations from culture media, or biological fluids such as serum, semen, urine,

etc., represent a pool of mixed EVs, with each subspecies having a different cargo and function. The cargo of the EVs contains important complex molecules such as RNA, DNA, proteins, lipids, and carbohydrates. The ratio of each subspecies and their molecular content may vary depending on the physiological/pathological status of the parent cells and tissues that release the EVs. Thus, EVs may potentially be a powerful source for noninvasive diagnosis of diseases (10).

The study by Freeman et al. (11) in this issue of *Diabetes* is unique in that it uses an ex vivo approach to study the role and mechanism of action of EVs derived from blood plasma of normal patients, patients with pre-diabetes, and patients with diabetes in the development of disease (11). The availability of plasma EVs from cohorts of individuals at two time points, separated by 5 years, allowed monitoring of changes associated with disease progression, since it was possible to compare individuals without diabetes with those who progressed to overt diabetes. The ex vivo approach is useful because it allows the investigation of the role of vesicles in disease in a quasi-prospective manner to monitor disease progression. Several of their findings were somewhat expected and actually served as a validation of published findings using in vitro systems. For example, they noted that the numbers of exosomes in the plasma correlated with disease severity (11). This has been observed in previous studies of diabetes (12,13). Thus, the more EVs present in the plasma, the more advanced the disease stage. Another interesting observation by Freeman et al. is that EVs from individuals with diabetes were preferentially internalized by monocytes and B cells, in contrast to EVs from normal euglycemic individuals. This led to an increase in cytokine secretion and activation of cell survival and oxidation signals (11), suggesting that the diabetes-related EVs may act as a proinflammatory trigger.

The study revealed a few rather unexpected findings. For example, the authors observed that patients with diabetes had significantly higher levels of erythrocyte-derived EVs as characterized by positivity for CD235. In addition,

<sup>1</sup>Biomedical Research Institute of Southern California, San Diego, CA

<sup>2</sup>The Scripps Research Institute, La Jolla, CA

Corresponding author: Yang D. Dai, [yddai@bri-sc.org](mailto:yddai@bri-sc.org).

© 2018 by the American Diabetes Association. Readers may use this article as long as the work is properly cited, the use is educational and not for profit, and the work is not altered. More information is available at <http://www.diabetesjournals.org/content/license>.

See accompanying article, p. 2377.

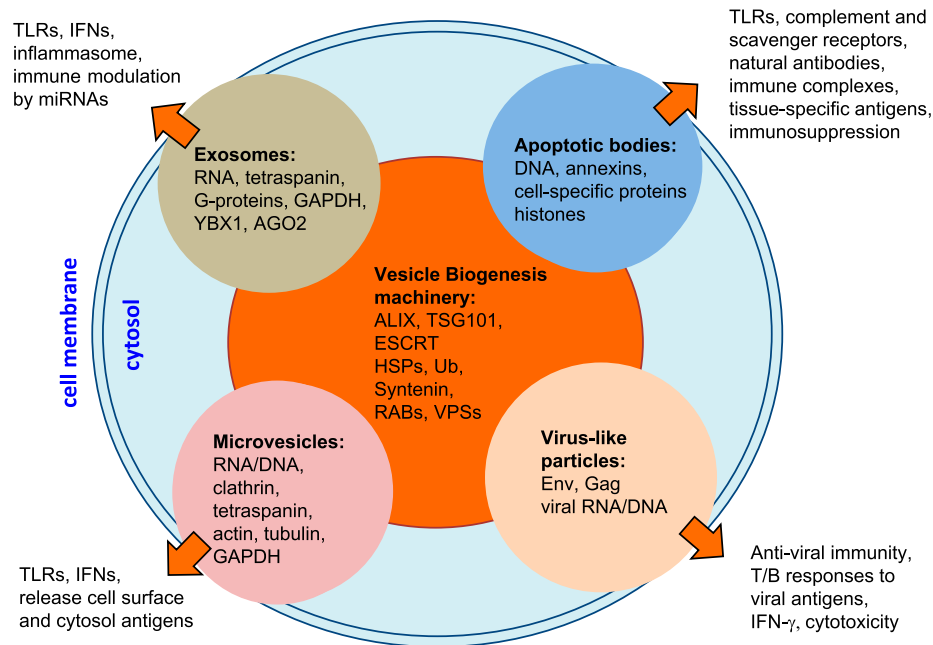


**Figure 1**—Characteristics of EVs and reactions of the immune system. The endosomal sorting machinery is central for generating different types of vesicles for secretion. Exosomes are formed from within the cytosol as multiple vesicle bodies, whereas microvesicles are formed near the plasma membrane via membrane budding (although they are the most closely related to exosomes) (27). Virus-like particles can be assembled and released by virus-infected cells or by cells that express endogenous retroviral proteins. Apoptotic bodies are released from cells undergoing programmed cell death. The molecular contents of the different types of vesicles or subset of EVs vary depending on cell of origin, status of activation, and cell fate, but there are many shared components, particularly those involving vesicle biogenesis and intracellular sorting. The immune responses listed for each type of vesicle are generalizations based on the limited knowledge in the field. This is because there are currently limited methods for separating the different subsets of vesicles and, consequently, few studies of the immune responses to EVs that would help to classify the responses to individual EV subsets. T/B, T-cell/B-cell.

their observation that the levels of insulin signaling proteins in the vesicles reflected the levels of insulin resistance and  $\beta$ -cell dysfunction merits further investigation. Furthermore, the authors argued that a hyperinsulinemic condition could increase an autophagy pathway resulting in the release of EVs; however, testing this hypothesis experimentally may require the use of an *in vivo* model of insulin resistance. Finally, the authors claimed that ultracentrifugation was a less reproducible method than the commercial kit for EV isolation. The approach for isolating EVs has been a controversial topic. Generally, the ultracentrifugation method is considered the gold standard for isolating exosomes (14). More recent studies have suggested that the use of commercial kits gives better yield and/or purity of EVs (15,16); however, Rider et al. (17) have shown that a newer approach described as ExtraPEG may even be better than the ultracentrifugation method and existing commercial kits and perhaps more economical. Ultimately, the choice of techniques for EV isolation may be determined by the desired EV subsets and/or molecular contents.

Future studies are required to dissect the antigenic materials in the EVs and to identify the innate and adaptive immune cells and molecular pathways that can react to the antigens. Heat-shock protein Hsp72, expressed in exosomes, can activate the Stat3 signaling pathway by inducing

IL-6 (18). Exosomes containing viral miRNAs may activate antiviral immune responses in dendritic cells (19). Depending on the types of antigens, exosomes may activate macrophages to secrete either TNF- $\alpha$  or IL-10, a functional polarization of the macrophages toward type 1 (M1) or type 2 (M2) cells, respectively. Adaptive immunity can be more potent than innate immunity in driving the polarization of the macrophages. It has been shown that dendritic cells function independently from macrophages to drive inflammation in adipose tissue, possibly by activating antigen-specific T cells (20). Innate lymphoid cells in adipose tissue (21) or islets (22) may respond to early antigens or inflammatory signals to further polarize the immune responses into different profiles. Sheng et al. (23) found that exosomes contain unique antigens that activate autoreactive T cells to produce type 1 T helper (Th1) cytokine IFN- $\gamma$ , possibly by first activating marginal zone-like B cells to present the antigens (24). Furthermore, retroviral antigens expressed in the vesicles may specifically induce antiviral immunity that could contribute to autoimmunity (25). Finally, genetic factors may determine the types of antigens expressed in the EVs and thus the types of immune responses that are induced. For example, adipose-derived stem cells release exosomes that drive macrophage differentiation into IL-10-secreting M2 cells (26). However, mesenchymal stem cells derived from autoimmune-prone mouse strain, NOD,

release exosomes that contain antigens that activate auto-reactive T cells to release the Th1 cytokine IFN- $\gamma$  (4). Therefore, a polarization of the immune responses toward a type 1 reaction to the EVs could be the driving force of  $\beta$ -cell damage and insulin resistance.

In summary, EVs are complex not only in shape, size, and molecular content but also in cell/tissue origin and function. As illustrated by Freeman et al. (11), the study of these vesicles will immensely enhance our understanding of the mechanisms of development of diseases and may provide novel methods for monitoring disease progression. One point that is clear is that EVs are produced in abundance in diseases such as cancers, autoimmune diseases, and viral infections. Unfortunately, there are currently no available technologies that can segregate EVs based on their origin or function. The ability to segregate EVs into subspecies based on their origin or function will significantly enhance our understanding of the pathology of several diseases, particularly autoimmune diseases.

---

**Duality of Interest.** No potential conflicts of interest relevant to this article were reported.

## References

- Mathis D. Immunological goings-on in visceral adipose tissue. *Cell Metab* 2013;17:851–859
- Lumeng CN, Saltiel AR. Inflammatory links between obesity and metabolic disease. *J Clin Invest* 2011;121:2111–2117
- Deng ZB, Poliakov A, Hardy RW, et al. Adipose tissue exosome-like vesicles mediate activation of macrophage-induced insulin resistance. *Diabetes* 2009;58:2498–2505
- Rahman MJ, Regn D, Bashratyan R, Dai YD. Exosomes released by islet-derived mesenchymal stem cells trigger autoimmune responses in NOD mice. *Diabetes* 2014;63:1008–1020
- Kranendonk ME, de Kleijn DP, Kalkhoven E, et al.; SMART Study Group. Extracellular vesicle markers in relation to obesity and metabolic complications in patients with manifest cardiovascular disease. *Cardiovasc Diabetol* 2014;13:37
- Jalabert A, Vial G, Guay C, et al. Exosome-like vesicles released from lipid-induced insulin-resistant muscles modulate gene expression and proliferation of beta recipient cells in mice. *Diabetologia* 2016;59:1049–1058
- Raposo G, Stoorvogel W. Extracellular vesicles: exosomes, microvesicles, and friends. *J Cell Biol* 2013;200:373–383
- Gould SJ, Booth AM, Hildreth JE. The Trojan exosome hypothesis. *Proc Natl Acad Sci U S A* 2003;100:10592–10597
- Anderson M, Kashanchi F, Jacobson S. Role of exosomes in human retroviral mediated disorders. *J Neuroimmune Pharmacol* 2018;13:279–291
- Laurent LC, Abdel-Mageed AB, Adelson PD, et al. Meeting report: discussions and preliminary findings on extracellular RNA measurement methods from laboratories in the NIH Extracellular RNA Communication Consortium. *J Extracell Vesicles* 2015;4:26533
- Freeman DW, Noren Hooten N, Eitan E, et al. Altered extracellular vesicle concentration, cargo, and function in diabetes mellitus. *Diabetes* 2018;67:2377–2388
- Salomon C, Scholz-Romero K, Sarker S, et al. Gestational diabetes mellitus is associated with changes in the concentration and bioactivity of placenta-derived exosomes in maternal circulation across gestation. *Diabetes* 2016;65:598–609
- Burger D, Turner M, Xiao F, Munkonda MN, Akbari S, Burns KD. High glucose increases the formation and pro-oxidative activity of endothelial microparticles. *Diabetologia* 2017;60:1791–1800
- Cvjetkovic A, Lötval J, Lässer C. The influence of rotor type and centrifugation time on the yield and purity of extracellular vesicles. *J Extracell Vesicles* 2014;3:10.3402/jev.v3.23111
- Rekker K, Saare M, Roost AM, et al. Comparison of serum exosome isolation methods for microRNA profiling. *Clin Biochem* 2014;47:135–138
- Helwa I, Cai J, Drewry MD, et al. A comparative study of serum exosome isolation using differential ultracentrifugation and three commercial reagents. *PLoS One* 2017;12:e0170628
- Rider MA, Hurwitz SN, Meckes DG Jr. ExtraPEG: a polyethylene glycol-based method for enrichment of extracellular vesicles. *Sci Rep* 2016;6:23978
- Chalmin F, Ladoire S, Mignot G, et al. Membrane-associated Hsp72 from tumor-derived exosomes mediates STAT3-dependent immunosuppressive function of mouse and human myeloid-derived suppressor cells. *J Clin Invest* 2010;120:457–471
- Baglio SR, van Eijndhoven MA, Koppers-Lalic D, et al. Sensing of latent EBV infection through exosomal transfer of 5'pppRNA. *Proc Natl Acad Sci U S A* 2016;113:E587–E596
- Cho KW, Zamarron BF, Muir LA, et al. Adipose tissue dendritic cells are independent contributors to obesity-induced inflammation and insulin resistance. *J Immunol* 2016;197:3650–3661
- O'Sullivan TE, Rapp M, Fan X, et al. Adipose-resident group 1 innate lymphoid cells promote obesity-associated insulin resistance. *Immunity* 2016;45:428–441
- Dalmas E, Lehmann FM, Dror E, et al. Interleukin-33-activated islet-resident innate lymphoid cells promote insulin secretion through myeloid cell retinoic acid production. *Immunity* 2017;47:928–942.e7
- Sheng H, Hassanali S, Nugent C, et al. Insulinoma-released exosomes or microparticles are immunostimulatory and can activate autoreactive T cells spontaneously developed in nonobese diabetic mice. *J Immunol* 2011;187:1591–1600
- Bashratyan R, Sheng H, Regn D, Rahman MJ, Dai YD. Insulinoma-released exosomes activate autoreactive marginal zone-like B cells that expand endogenously in prediabetic NOD mice. *Eur J Immunol* 2013;43:2588–2597
- Bashratyan R, Regn D, Rahman MJ, et al. Type 1 diabetes pathogenesis is modulated by spontaneous autoimmune responses to endogenous retrovirus antigens in NOD mice. *Eur J Immunol* 2017;47:575–584
- Zhao H, Shang Q, Pan Z, et al. Exosomes from adipose-derived stem cells attenuate adipose inflammation and obesity through polarizing M2 macrophages and beiging in white adipose tissue. *Diabetes* 2018;67:235–247
- van Niel G, D'Angelo G, Raposo G. Shedding light on the cell biology of extracellular vesicles. *Nat Rev Mol Cell Biol* 2018;19:213–228